

# REPORT

**Contract: 11245 UEP II**  
Final version, **Date: 21.08.2013**

Cicerstr. 24  
D-10709 Berlin  
Germany  
Tel +49 (0)30 536 53 800  
Fax +49 (0)30 536 53 888  
[www.kompetenz-wasser.de](http://www.kompetenz-wasser.de)

## Guidelines for the use of online fouling monitoring in tertiary treatment Project acronym: OXERAM 2

by  
Morgane Boulestreau  
Ulf Miehe

for  
Kompetenzzentrum Wasser Berlin gGmbH  
Cicerostrasse 24., 10709 Berlin, Germany

Preparation of this report was financed through funds provided by Berliner Wasserbetriebe, Veolia Water and Berlin Environmental Relief Programme (ERP)



Project co-financed by the  
Berlin Senate and the  
European Union.  
(European Regional  
Development Fund)  
Investing in your Future!



Senate Department  
for Urban Development  
and the Environment

**be:m:m Berlin**

Berliner  
Wasserbetriebe

Berlin, Germany

2013



## **Important Legal Notice**

**Disclaimer:** The information in this publication was considered technically sound by the consensus of persons engaged in the development and approval of the document at the time it was developed. KWB disclaims liability to the full extent for any personal injury, property, or other damages of any nature whatsoever, whether special, indirect, consequential, or compensatory, directly or indirectly resulting from the publication, use of application, or reliance on this document. KWB makes no guarantee or warranty, expressed or implied, as to the accuracy or completeness of any information published herein. It is expressly pointed out that the information and results given in this publication may become out of date due to subsequent modifications. In addition, KWB disclaims and makes no warranty that the information in this document will fulfil any of your particular purposes or needs. The disclaimer on hand neither seeks to restrict nor to exclude KWB's liability under relevant national statutory provisions.

## **Wichtiger rechtlicher Hinweis**

**Haftungsausschluss:** Die in dieser Publikation bereitgestellte Information wurde zum Zeitpunkt der Erstellung im Konsens mit den bei Entwicklung und Anfertigung des Dokumentes beteiligten Personen als technisch einwandfrei befunden. KWB schließt volumnäßig die Haftung für jegliche Personen-, Sach- oder sonstige Schäden aus, ungeachtet ob diese speziell, indirekt, nachfolgend oder kompensatorisch, mittelbar oder unmittelbar sind oder direkt oder indirekt von dieser Publikation, einer Anwendung oder dem Vertrauen in dieses Dokument herrühren. KWB übernimmt keine Garantie und macht keine Zusicherungen ausdrücklicher oder stillschweigender Art bezüglich der Richtigkeit oder Vollständigkeit jeglicher Information hierin. Es wird ausdrücklich darauf hingewiesen, dass die in der Publikation gegebenen Informationen und Ergebnisse aufgrund nachfolgender Änderungen nicht mehr aktuell sein können. Weiterhin lehnt KWB die Haftung ab und übernimmt keine Garantie, dass die in diesem Dokument enthaltenen Informationen der Erfüllung Ihrer besonderen Zwecke oder Ansprüche dienlich sind. Mit der vorliegenden Haftungsausschlussklausel wird weder bezweckt, die Haftung der KWB entgegen den einschlägigen nationalen Rechtsvorschriften einzuschränken noch sie in Fällen auszuschließen, in denen ein Ausschluss nach diesen Rechtsvorschriften nicht möglich ist.

## **Colophon**

Present report was developed in compliance with the requirements of the quality management system DIN EN ISO 9001:2008

Title

Guidelines for the use of online fouling monitoring in tertiary treatment

Authors

Boulestreau Morgane, KWB

Miehe Ulf, KWB

Quality Assurance

M. Jekel, FG Wasserreinhaltung, TU Berlin

M. Ernst, TU Hamburg-Harburg

U. Miehe, Kompetenzzentrum Wasser Berlin gGmbH

Publication / Dissemination approved by technical committee members:

C. Bourdon, Veolia

A. Tazi-Pain, Veolia

C. Bartholomäus, Berliner Wasserbetriebe

R. Gnirß, Berliner Wasserbetriebe

A. Peter-Fröhlich, Berliner Wasserbetriebe

M. Jekel, FG Wasserreinhaltung, TU Berlin

A. Hartmann, Kompetenzzentrum Wasser Berlin gGmbH

Deliverable number

D 3.1

Final version

Date: 21.08.2013

## Abstract (English)

Various tertiary treatment processes were compared in the OXERAM project, including a polymeric membrane and a microsieve pilot plant which were installed at the Ruhleben WWTP in Berlin and operated for almost two years. To increase the performance of both these processes, pre-treatments with ozonation, coagulation and/or flocculation were tested. In order to optimize the hybrid processes and to develop a control strategy, online monitoring was implemented. After a literature review and lab trials at the Technische Universität Berlin (TUB) during the project preparation phase, two instruments were recommended.

An NS500 device by Nanosight was installed in the UF membrane pilot (pore diameter = 20 nm) influent with sampling every 15 minutes before and after the inline coagulation. The particles between 50 and 1000 nm were analysed to evaluate the impact of the ozonation / coagulation or the coagulation alone on the nanoparticles below 500 nm which are most responsible for fouling. For a better reproducibility and quality of the results, samples were pre-filtered by an online metallic 5 µm filter. Particle analysis by Nanoparticle Tracking Analysis (NTA) was obtained to give reliable and reproducible information about the concentration and size distributions of the colloidal fraction in the tested treated domestic wastewater. Correlation between the membrane reversible fouling measured with the help of the trans-membrane pressure (TMP) and the concentration of particles between 100 and 200 nm were detected. Online measurements at the pilot-scale indicate that colloid peak concentrations can be compensated for by coagulation with an optimum dose of 8 mg Fe<sup>3+</sup>/L. Furthermore, a comparison of FeCl<sub>3</sub> and PACl demonstrated that the former is more effective in colloid removal in this treated domestic wastewater. Due to the combination of pre-ozonation and subsequent coagulation, a synergy effect was determined as the combined treatments lead to a better particle removal compared to the effect of the single treatments at same dosages of O<sub>3</sub> and Fe<sup>3+</sup>. A combination of 0.5 mg O<sub>3</sub>/mg DOC<sub>0</sub> and 8 mg Fe<sup>3+</sup>/L leads to a total reduction down to < 5 % of the initial colloid content<sup>1</sup>. However a direct prediction of irreversible fouling was not possible. This device should be further optimized for its potential to reduce operational costs and lower solid loads and thus fouling on the membrane.

A Pamas particle counter device was installed in the microsieve effluent pipe bypass and this measured the particle size distribution continuously by light extinction at a wavelength of 635 nm at 25 mL/min. No pre-treatment was necessary and it was possible to automatically clean the instrument every hour with distilled water or another cleaning solution. Piping and sensor cell maintenance was crucial to improve the quality of the results due to the high potential of the effluent water to post-flocculate. For optimization of the coagulant and flocculant mixing velocity, the particle counter results were more accurate than the turbidity sensor which did not detect any changes in the effluent water quality. The monitoring tool detected the lowest particle concentration for the optimized mixing velocity. However, the particle counter did not provide better information than an online turbidity sensor for other parameters such as the coagulant types or doses. Therefore, while it is recommended to use an online particle counter during the microsieve plant (10 µm) start-up phase to optimize the coagulation and flocculation, for routine controls an online turbidity sensor is sufficient. Moreover turbidity sensors are less

---

<sup>1</sup> we suggest to call the optimum "Schulz optimum" but transferability on other secondary effluent or surface water needs to be proven

demanding in terms of maintenance effort. The project showed that using the turbidity signal to adapt the coagulant dose was very efficient.

## Contents

Colophon .....	ii
Abstract (English).....	iii
Chapter 1 Introduction .....	1
Chapter 2 Particle separation and fouling.....	2
2.1 Colloids/Particles/flocs .....	2
2.1.1 Definitions .....	2
2.1.2 Particle size .....	2
2.1.3 Number/surface/volume distribution.....	3
2.1.4 Cumulative/differential distribution .....	4
2.2 Particle behaviour during ozonation, inline coagulation and membrane filtration.....	4
2.2.1 Effect of ozonation .....	4
2.2.2 Effect of coagulation.....	5
2.2.3 Effect of ozonation followed by coagulation.....	5
2.2.4 Effect of membrane filtration: mechanism, fouling .....	6
2.3 Particle behaviour during coagulation, flocculation and micro sieve filtration .....	6
2.3.1 Effect of coagulation and flocculation.....	7
2.3.2 Effect of micro sieve filtration: mechanism, fouling .....	7
Chapter 3 Monitoring of membrane fouling .....	9
3.1 Selection of the suitable device.....	9
3.2 Materials and methods .....	9
3.2.1 Nanoparticle tracking analysis: design of device, measuring principle.....	9
3.2.2 Lab equipment (Genz et al., 2011) .....	12
3.2.3 Fouling analysis (see Appendix 2).....	14
3.2.4 Pilot plant: online implementation .....	14
3.3 Lab results.....	16
3.3.1 Reproducibility and reliability of the device.....	16
3.3.2 Effect of ozonation and coagulation on effluent water quality .....	16
3.3.3 Relationship between Nanosight results and Amicon cell filtration performance .....	19
3.3.4 Determination of effluent composition with scattering intensity measurement (Appendix 3) .....	22
3.4 Online results.....	22
3.4.1 Seasonal and daily variations .....	23
3.4.2 Effect of coagulation on effluent water quality .....	25

3.4.3 Relationship between submicron particles and filtration behaviour .....	27
3.5 Comparing Nanosight results with other parameters .....	29
3.5.1 Submicron particles and other analytical parameters.....	29
3.5.2 Dissolved organic carbon (DOC) .....	30
3.5.3 Liquid Chromatography - Organic Carbon Detection (LC-OCD).....	30
3.6 Operational experiences.....	31
3.7 Conclusion on online monitoring of membrane fouling.....	32
Chapter 4 Monitoring of micro sieve performances .....	35
4.1 Selection of the suitable device .....	35
4.2 Materials and methods.....	35
4.2.1 Particle counter: characteristics, principle of light extinction .....	35
4.2.2 Lab equipment .....	37
4.2.3 Pilot plant: online implementation.....	38
4.3 Lab results .....	38
4.3.1 Reproducibility and reliability of the device .....	38
4.3.2 Comparing influent and effluent water quality .....	39
4.3.3 Comparison of coagulant type: iron and aluminium, effect of pH .....	39
4.3.4 Postflocculation analysis.....	40
4.3.5 Fractionation tests .....	42
4.4 Pilot plant results .....	43
4.4.1 Results repeatability .....	43
4.4.2 Influence of the influent flow .....	44
4.4.3 Effluent water quality with and without pre-treatments.....	45
4.4.4 Optimization of the coagulation: type, dose, mixing and hydraulic retention time ....	46
4.4.5 Optimization of the flocculation: type, dose, mixing and hydraulic retention time ....	48
4.5 Operational experiences.....	51
4.6 Conclusion on online monitoring of microsieve performance .....	52
Appendix A Software options .....	53
Appendix B Fouling analysis.....	54
Appendix C Scattering intensity .....	56
Bibliography .....	58

## List of Figures

Figure 1: Common materials retained by membrane filtration adapted from (Crittenden, 2005; Melin and Rautenbach, 2004) .....	2
Figure 2: Projected area equivalent diameter of an irregular shaped particle .....	3
Figure 3: Cumulative size distribution of number and volume of particles contained in a secondary effluent measured with a particle counter.....	3
Figure 4: Design of NanoSight NS500 device (right) and the contained viewing unit (left).....	10
Figure 5: Schematic illustration of the optical path of the laser beam and the detection objective .....	10
Figure 6: a) Normalized colloid content (NTA) versus the specific ozone dosage, b) impact of the ozone on the size distribution of colloidal and dissolved organic matter (LCOCD) .....	17
Figure 7: Normalized colloid content vs. the applied Fe dosage: a) total particle content, b) particle < 200 nm.....	18
Figure 8: Impact of pre ozonation and subsequent coagulation on the submicron particle content a) size distribution, b) particle removal < 200 nm at different ozone and coagulant dosages.....	18
Figure 9: Impact of pre-ozonation and subsequent coagulation on: a) total fouling resistance normalized to the untreated sample, b) concentration of colloid fractions and corresponding total fouling resistance .....	20
Figure 10: Impact of pre-ozonation and subsequent coagulation on: a) irreversible fouling resistance normalized to the untreated sample, b) concentration of colloid fractions and corresponding irreversible fouling resistance .....	21
Figure 11: Variations of submicron particle content in the secondary treated Ruhleben effluent, including grab samples taken between 8.30 a.m. and 10.00 a.m. (n=34), 24h mixed samples (n=27), daily mean values of online measurements (n=42), and weather data for Berlin Tegel during this study ( <a href="http://www.dwd.de">www.dwd.de</a> ) .....	23
Figure 12: Daily variation of wastewater inflow to WWTP Ruhleben and corresponding total particle concentration and turbidity in the effluent .....	24
Figure 13: Colloid removal (< 200 nm) by coagulation in the UF-pilot unit: a) Behaviour of colloid removal in dependence to initial concentration, b) comparison of removal by different coagulants (FeCl <sub>3</sub> , PACl).....	25
Figure 14: Development of the normalized starting permeability after each backwash of the UF-pilot unit at trials with three different coagulant dosages between 17 October and 1 December 2011.....	26
Figure 15: Development of total fouling resistance per filtration cycle and corresponding online measured concentration of colloidal fraction (< 200 nm) of coagulated secondary effluent (1.9 mg Al <sup>3+</sup> /L).....	27
Figure 16: Relationship between colloid concentration of different fractions after coagulation by 1.9 mg Al <sup>3+</sup> /L and a) total fouling resistance, b) irreversible fouling resistance, c) relationship between particle load and long term irreversible fouling during a UF-filtration trial .....	28
Figure 17: Principle of light extinction.....	36
Figure 18: Jar-Test apparatus .....	37
Figure 19: Picture of the particle counter in the pilot plant .....	38
Figure 20: Standard particles (50 µm) at different concentrations: a) number, b) volume distribution .....	38

Figure 21: Postflocculation experiments without automatic cleaning a) 26.10.10, b) 27.10.10, c) 28.10.10 .....	41
Figure 22: Postflocculation experiments with automatic cleaning .....	42
Figure 23: Lab analysis results of the fractionation tests a) TP, b) residual Al, c) filterability .....	42
Figure 24: Differential particle count results of the fractionation test for particle sizes between 43 .....	43
Figure 25: Impact of the influent flow on the effluent water quality.....	44
Figure 26: Impact of the influent flow on the effluent water quality.....	45
Figure 27: Impact of the pre-treatments on the effluent water quality. ....	46
Figure 28: Particle count for an increasing a) iron chloride dose and b) polyaluminium chloride dose.....	46
Figure 29: Increase of the mixing velocity in the coagulation tank .....	48
Figure 30: Impact of chemicals doses increase on the effluent water quality .....	49
Figure 31: Impact of the flocculant type on the total particle count in the microsieve effluent ..	50
Figure 32: Increase of the mixing velocity in the flocculation tank .....	50
Figure 33: Particle counter piping system fouled .....	51
Figure 34: Relation between particle size and scattering intensity of different particle standard (PS) materials compared to intensity signal of a secondary effluent (SE) sample .....	56

## List of Tables

Table 1: Standard protocol settings for submicron particles analysis with the NS500 device .....	12
Table 2: Analytical methods for characterization of water quality.....	13
Table 3: Selected results of the correlation analysis (R = Pearson correlation coefficient; p = 0.05) .....	29
Table 4: Organic substances size and weight distribution (modified after Crittenden et al., 2005, Filloux, 2006, Hofmann & Kammer, 2009) .....	30
Table 5: Correlation between LC-OCD and Nanosight results.....	31
Table 6: Characteristic of the WaterViewer .....	35
Table 7: Particle count and particle removal before and after Jar-Testing.....	39
Table 8: Comparison of particle count for different coagulant types at different pH .....	40
Table 9: Particle counter repeatability.....	43

## List of Equations

Equation 1: Stokes-Einstein equation.....	11
equation 2: Darcy's law.....	54
equation 3: initial membrane resistance .....	54
equation 4: total fouling resistance .....	54
equation 5: irreversible fouling.....	54
equation 6: reversible fouling.....	54
equation 7: fouling rate .....	55

## Abbreviations and symbols

### Abbreviations

BDOC	[mg L <sup>-1</sup> ]	biological degradable organic carbon
BOD	[mg L <sup>-1</sup> ]	biological oxygen demand
BW	-	backwash
CA	-	cellulose acetate
CCD	-	charged-coupled device
CE	-	cellulose ester
CEB	-	chemically enhanced backwash
CIP	-	cleaning in place
cfu	[mL <sup>-1</sup> ]	colony-forming units
COD	[mg L <sup>-1</sup> ]	chemical oxygen demand
DLS	-	dynamic light scattering
DOC	[mg L <sup>-1</sup> ]	dissolved organic carbon
ENP	-	engineered nanoparticles
EOM	-	extracellular organic matter
FTC	-	flow through cell
HRT	[sec]	hydraulic retention time
ICP-OES	-	inductively coupled plasma – optical emission spectroscopy
LC-OCD	-	liquid chromatography with organic carbon detection
LOD	-	limit of detection
LOQ	-	limit of quantification
MAC	[g m <sup>-3</sup> ]	maximum allowable concentration
MBR	-	membrane bioreactor
MF	-	microfiltration
MW	[g mol <sup>-1</sup> ]	molecular weight
MWCO	[g mol <sup>-1</sup> ]	molecular weight cut off
NF	-	nanofiltration
NOM	[mg L <sup>-1</sup> ]	natural organic matter
NTA	-	nanoparticle tracking analysis
NTU	-	nephelometric turbidity unit
PA	-	polyamide
PAC	-	powdered activated carbon
PACl	-	polyaluminium chloride
PES	-	polyethersulphone
PSA	-	pressure swing adsorption
PVC	-	polyvinyl chloride
PVDF	-	polyvinylidene fluoride
RO	-	reverse osmosis
rpm	-	revolutions per minute
SE	-	secondary treated effluent
SEC	-	size exclusion chromatography
SP	-	sampling point

SS	[mg L <sup>-1</sup> ]	suspended solids
TMP	[bar]	trans-membrane pressure
TOC <sub>5μm</sub>	[mg L <sup>-1</sup> ]	total organic carbon after 5 μm filtration
TUB	-	Technische Universität Berlin
UF	-	ultrafiltration
UVA <sub>254</sub>	[1 m <sup>-1</sup> ]	UV-absorbance at 254 nm
WWTP	-	wastewater treatment plant

## Symbols

### *Latin symbols*

c	[mg L <sup>-1</sup> ]	concentration
c <sub>f</sub>	[mg L <sup>-1</sup> ]	feed concentration of a solute
c <sub>p</sub>	[mg L <sup>-1</sup> ]	permeate concentration of a solute
c <sub>r</sub>	[mg L <sup>-1</sup> ]	retentate concentration of a solute
d	[m]	hydrodynamic diameter
d <sub>p</sub>	[m]	spherical diameter
d <sub>pore</sub>	[m]	mean pore diameter
D <sub>t</sub>	[m <sup>2</sup> s <sup>-1</sup> ]	diffusion coefficient
G	[s <sup>-1</sup> ]	velocity gradient
J	[L m <sup>-2</sup> h <sup>-1</sup> ]	flow rate/flux through the membrane
J <sub>0</sub>	[L m <sup>-2</sup> h <sup>-1</sup> ]	pure water flux
k	[M <sup>-1</sup> s <sup>-1</sup> ]	reaction constant
k <sub>B</sub>	[J K <sup>-1</sup> ]	Boltzmann constant (1.3806488 x10 <sup>-23</sup> )
K <sub>w</sub>	[L m <sup>-2</sup> h <sup>-1</sup> bar <sup>-1</sup> ]	membrane permeability
m <sub>x</sub>	[mg min <sup>-1</sup> ]	mass flow component x
M	[g mol <sup>-1</sup> ]	molecular weight
p	[Pa]	pressure
P	[Nm s <sup>-1</sup> ]	mechanic power
r	[m]	spherical radius
R	[%]	retention rate
R <sub>d</sub>	[m <sup>-1</sup> ]	total fouling resistance
R <sub>f</sub>	[m <sup>-1</sup> ]	total hydraulic filtration resistance
R <sub>m</sub>	[m <sup>-1</sup> ]	membrane resistance
R <sub>rev</sub>	[m <sup>-1</sup> ]	reversible fouling resistance
R <sub>irr</sub>	[m <sup>-1</sup> ]	irreversible fouling resistance
t	[s]	time
T	[°C]	temperature
V	[m <sup>3</sup> ]	volume
V <sub>f</sub>	[m <sup>3</sup> ]	filtration volume
Z <sub>O<sub>3</sub></sub>	[mg L <sup>-1</sup> ]	ozone consumption

### *Greek symbols*

β	-	blocking law filtration coefficient, unit varies depending on φ
δ	[m]	surface distance
κ	[μS cm <sup>-1</sup> ]	electrical conductivity
η	[m <sup>2</sup> s <sup>-1</sup> ]	dynamic viscosity
ϕ	[-]	blocking law filtration exponent
σ	[-]	standard deviation

## **Chapter 1 Introduction**

The Oxeram project aimed at the development of a cost and energy efficient advanced tertiary wastewater treatment. The project remit was to identify the most sustainable solution for meeting the goals of the European Water Framework Directive and ensuring the bathing water quality in Berlin's surface waters. Among other solutions, Oxeram assessed membrane filtration pre-treated with ozonation and coagulation and microsieve filtration pre-treated with coagulation and flocculation. One objective was to develop a new strategy for online monitoring of these processes. The recommended monitoring tools of the preparation phase project were implemented and optimized to characterize the tertiary filtration processes and the pre-treatments effects on their performances. Online monitoring is a powerful tool to optimize processes. One goal was to assess the resultant membrane fouling and the microsieve performance. The final goal was to couple the online monitoring results with the pre-treatment types and doses for rapid and dynamic process optimization. The availability of such sensors would strongly improve the operation of filtration systems as they would make it possible to minimize costs and operation risks such as membrane fouling.

This report presents the implementation of the Nanosight device in the polymeric membrane (UF) pilot plant. This tool is based on nanoparticle tracking analysis (NTA) method and commercialized in Germany by the company NanoSight Ltd. The particle size distribution between 50 and 1000 nm in the Ruhleben WWTP effluent wastewater was analysed first at lab scale and then automatically every 15 minutes before and after coagulation in the pilot plant. The KWB was one of the first companies to buy this innovative device and the first company to implement it online to obtain information on pilot plant operation. The goal was to find the operating conditions under which the particle number below 500 nm (important foulants) was minimized.

A second device based on light extinction, a particle counter, was implemented in the microsieve pilot plant. The particle counter "Waterviewer" provided by the Pamas company counts the particles between 1 and 200 µm in the microsieve effluent wastewater, providing a particle size distribution for eight different size ranges. Samples were continuously pumped from the effluent pipes to the sensor cell and automatic cleaning took place every hour for example with distilled water. The exploitation was rapid (-30s) and the time could be chosen by the operator. The objective was to find out under which operating conditions the particle concentration in the effluent of the microsieve was the lowest, offering the best effluent quality together with good filtration performance.

Both the instruments tested in pilot plant provided a particle size distribution, which is the easiest parameter to analyse online because it allows a 3D object to be defined by one number, assuming that particles are spherical. In addition to the online monitoring, several parameters such as dissolved organic carbon or LC-OCD were analysed in the lab to find correlations between the substances in the wastewater, their sizes, and their effects on filtration performances. Organic compounds are known to foul membranes more than inorganic ones.

The following chapter will define the water compounds and their distribution in more detail and will describe the influence on these substances of pre-treatments like ozonation, coagulation and flocculation. The third and the fourth chapter will present the membrane fouling monitoring and the microsieve performance monitoring respectively. Finally conclusions and recommendations are provided.

## Chapter 2 Particle separation and fouling

### 2.1 Colloids/Particles/flocs

#### 2.1.1 Definitions

Water constituents are of very different origin and appear in a large variety of sizes, shapes, density, mobility, sedimentation velocity, shear strength, and various chemical properties (surface, composition, and adsorption).

A particle is a water element defined by its size. The limits between dissolved matter, colloidal and suspended material are problematic. The limit between colloids and suspended material is set to 1  $\mu\text{m}$  (Gregory, 2004; Ljunggren, 2004). The limit between dissolved matter and colloids is arbitrarily defined by a filtration at 0.45  $\mu\text{m}$  (EN 1484, 1997). See Figure 1.

Floc refers in this work to a group of aggregated particles. The size of flocs range from  $\mu\text{m}$  to a few mm.

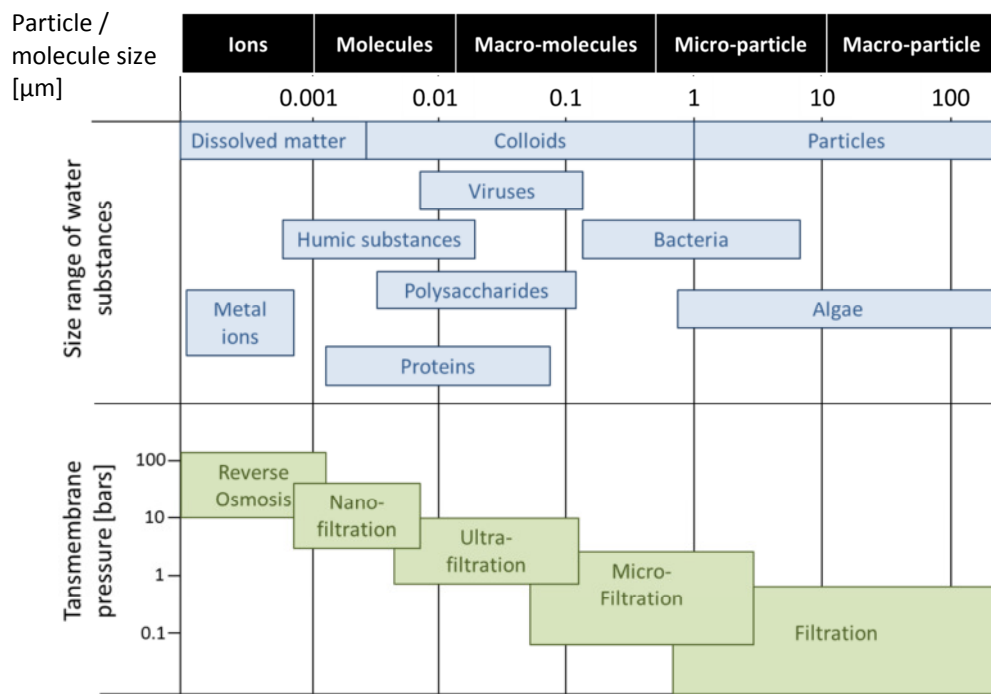


Figure 1: Common materials retained by membrane filtration adapted from (Crittenden, 2005; Melin and Rautenbach, 2004)

#### 2.1.2 Particle size

Detailed analysis of the particle numbers includes the evaluation of the particle size. A coarse indication of the size range of some well-known particle classes is given in Figure 1.

The size of particles in water is strongly dependent on particle origin and history as well as on the flow regime (Nieuwenhuijzen A., 2011). The size is not easy to determine, so it is often expressed as an equivalent diameter. Particle size is defined by the particle diameter, which aims at comparing the dimension of the particles with just one number, assuming that particles are spherical, although most of the particles have an irregular shape.

An equivalent diameter is reported as the diameter of a sphere having the same value of a specific property (e.g. Brownian and electrical motion, light scattering, projected area, mass) as the irregularly shaped particle being measured.

The mobility/diffusion equivalent diameter was calculated for particles < 1  $\mu\text{m}$  analyzed by the nanoparticle tracking analysis (NTA). It is the diameter of a sphere with the same mobility (Brownian motion) as the particle in question.

For particles in the micron range measured by particle counter, the surface equivalent diameter was calculated. It is the diameter of a sphere with the same projected cross-sectional area as the particle in question. See Figure 2 (Nieuwenhuijzen A., 2011).

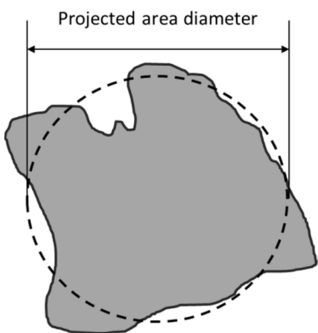


**Figure 2: Projected area equivalent diameter of an irregular shaped particle**

### 2.1.3 Number/surface/volume distribution

To characterize the particle size for an ensemble of particles, the concept of particle size distribution is introduced. It reflects the polydispersity of the sample analysed.

The particle size distribution is the particle number which diameter is the equivalent diameter defined in the previous chapter per volume (#/mL). The number of particles of different sizes normally decreases with increasing particle size in wastewater suspensions.

For the particle surface/volume distribution, the surface/volume of a particle is calculated as the surface/volume of a sphere which diameter is the equivalent diameter. The volume distribution reflects the polydispersity of the samples in term of place occupied by the particles. See Figure 3.

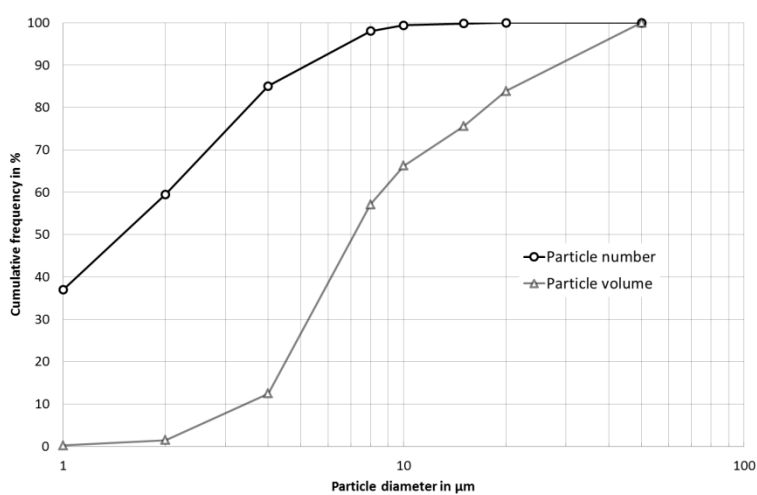


**Figure 3: Cumulative size distribution of number and volume of particles contained in a secondary effluent measured with a particle counter**

#### **2.1.4 Cumulative/differential distribution**

The differential distribution shows the relative particle amount in each particle size range. The cumulative size distribution displays the particle fraction below or above a series of specific sizes. The differential distribution is the first derivative of the cumulative distribution. To obtain the cumulative distribution, the differential distribution is integrated.

### **2.2 Particle behaviour during ozonation, inline coagulation and membrane filtration**

In this chapter colloids and organic matter (OM) will be of particular interest. Colloids are the submicron particles mostly responsible for membrane fouling because their size in the nanometre range ( $1\text{ nm} \sim 500\text{ Da}$ ) is in the same range as the membrane pore size studied in the OXERAM project: 20 nm for the polymeric ultrafiltration membrane and 100 nm for the ceramic microfiltration membrane. Colloids sometimes behave like dissolved substances, but also like particles. Organic matter is a complex mixture of degradation products of a great variety of natural compounds which incorporates proteins, polysaccharides and lipids. Organic matter has specific properties which can interact with the membrane surface or with the others compounds in water. These interactions are not completely understood and lead to irreversible fouling of low pressure membranes.

#### **2.2.1 Effect of ozonation**

Colloids have a large specific surface area, and hence their properties are dominated by surfaces rather than bulk. The active surface of a particle or a macromolecule per volume unit increases with decreasing particle size. Since ozonation changes the surface characteristics of particles, it has a high impact on colloids and organic matter.

Ozonation oxidizes organic compounds by two reactions (Moulin, 1990): reactions with electron rich structure (aromatic groups and unsaturated and nitrogenous aliphatic groups) and reactions via radicals such as  $\text{HO}^\bullet$ ,  $\text{O}_2^\bullet$  and  $\text{HO}_2^\bullet$  which are very reactive and less selective than molecular ozone. It can degrade natural organic matter and enhance the transformation of higher molecular weight compounds into lower molecular weight ones. The apparent molar mass is modified: high molecular weights are decreased and low molecular weights are increased (Zhu et al., 2008). This modification in the particle distribution of water depends strongly on the ozone dose applied.

The oxidation of organic compounds makes them more polar by the introduction of COOH groups. They are then more easily biodegradable. Oxidized organic compounds are more soluble in the water and hydrophilic, poorer in ethylenic liaison, lower in molecular weight (Roustan et al., 1980; Zhu et al., 2008).

*Ozone + membrane:*

*The ozonation has an effect on the particle size depending on the ozone dose and the membrane used which can either be beneficial for the filtration if smaller particles pass through the membrane, or detrimental if smaller particles block the membrane pores.*

*The ozonation has an effect on the particle properties (compounds more hydrophilic) which influence the fouling by altering the chemical interactions between the membrane material and foulants (Roustan et al., 1980; Zhu et al., 2008).*

## 2.2.2 Effect of coagulation

During this study, coagulation was used to remove colloids and suspended materials, to precipitate phosphate and to reduce larger dissolved organic compounds such as biopolymer and humic substances. However coagulation alone is not enough, another treatment step is needed for the liquid/solid separation process. It can be the addition of organic polymer to create larger flocs followed by sedimentation or microsieve filtration; or the coagulation is used as pretreatment for low pressure membrane filtration to limit membrane fouling.

In the OXERAM project, aluminium-based and ferric-based coagulants were used at doses between 1 and 12 mg Me/L with a pH around 7. These coagulants are the most commonly applied coagulation agents in water and wastewater treatment. At pH ranges between 6.5 – 9.0 for ferric and 6.0 – 7.0 for aluminium, they form insoluble neutral species ( $\text{Me(OH)}_3$ ) in case of sweep coagulation. The insoluble neutral species precipitate and enclose dispersed compounds into flocs. A reaction with organic compounds is also possible and an additional coagulant consumption proportional to the DOC will occur (Jekel, 1998; Schulz, 2012). The cationic metal interacts electrostatically with the anionic NOM to form insoluble charge-neutral products which can then agglomerate themselves.

In practice there are various mechanisms depending on the concentration and type of coagulant, the DOC and the concentrations and nature of colloid and the pH (Bache and Gregory, 2007, 2010). But the coagulation process goal is always to destabilize and aggregate dispersed water ingredients and precipitate dissolved organic and inorganic compounds (Jekel, 2004). Another coagulation mechanism is to reduce the energy barrier between colloids: the double layer around the particle/colloid is decreased with the increase of the ionic strength. Aluminium-based and ferric-based coagulants are known to preferentially remove hydrophobic rather than hydrophilic substances, charged rather than neutral substances, and larger rather than smaller sized substances.

### *Coagulation + membrane:*

*Coagulation changes particle characteristics such as size, charge and shape (Kim et al. 2005). The goal of the coagulation is to increase the particle size to have a ratio particle diameter/pore size of the membrane > 10. The hybrid system coagulation/membrane filtration increases the permeate flux. This increase is due to a decrease in the resistance cake and less irreversible fouling. Coagulated colloids form a porous low-density cake layer, which is easily removed by backwash (Meier et al., 2006; NAN et al., 2008; Leiknes, 2009; Soun-Ok Baek, 2009; Stoller, 2009).*

## 2.2.3 Effect of ozonation followed by coagulation

Ozone can shift particle size distributions towards larger sizes by influencing interactions between dissolved organic matter and coagulant. Ozonation of organic matter increases oxygenated functional groups on the surface of particles, especially the carboxylic acids. Organic compounds with acid functional groups are better adsorbed by flocs. Then the metallic ions act as bridges to make particles grow into larger one (Langlais, 1991; You, 2007; Moulin, 1990).

Ozonation can lead to organic desorption from mineral particle surfaces through decreasing molecular weight or increasing hydrophilicity of organic matters. The loss of the organic matter from surface decreases the repulsive force between particles and so increases the possibility of

particles colliding and accreting. The break-up of organometallic complexes creates metallic salts, which can act as flocculants (Richard, 1980). The surface charge of the particles is changed, the particle destabilization is induced by reducing steric and electrostatic barriers, and finally the average particle size increases due to agglomeration (Boulestreau, 2009).

Low ozone dose is the most effective of the coagulating effects. With increasing ozone dosages, the coagulation-aid effect gradually disappears as the molecules become smaller with ozonation and no more bridge effects occur. A low ozone demand is also important to make the process economical in comparison with conventional treatments (Jekel, 1998). Singer (1990) suggests the dosage of pre-ozonation for best coagulation is between 0.4 and 0.8 mg O<sub>3</sub>/mg DOC<sub>0</sub>.

#### **2.2.4 Effect of membrane filtration: mechanism, fouling**

The main disadvantage of the membrane filtration is fouling (increase of filtration resistance). There are different types of fouling, mainly reversible and irreversible fouling. It can be hydraulically reversible, or chemically reversible, or completely irreversible. Studies show that proteins and polysaccharides, also called biopolymers, are the most relevant substances in the irreversible fouling of the membranes. They are responsible for the diminution of the membrane life span due to more chemically cleaning and lead to a higher investment cost. A larger surface membrane and more frequent membrane replacements are required due to the loss of the membrane permeability. Lipp et al. (2009) show that inorganic particles are less responsible for fouling than organic particles of the same size. Similar results were found by Potts et al. (1981); Cheryan (1988), the dissolved organic matter was more responsible for the irreversible fouling than the colloid fraction (< 1 µm) or the particulate fraction (> 1 µm). This is partly due to the dissolved organic matter size compared to the membrane pore size: the foulant diameter is similar to the membrane pore diameter, which leads to pore blocking and adsorption of compounds into the membrane pores. The fouling mechanisms depend of the foulant size. If the foulant diameter / pore diameter ratio is less than 0.1, the adsorption of organic matter at the membrane surface may be statistically significant. If the foulant diameter / pore diameter ratio is greater than 10, the fouling is due to the formation of a cake layer at the membrane surface. Otherwise, fouling is by pore blocking (Crittenden, 2005; Stoller, 2009).

This information highlights the importance of foulant size monitoring to understand the fouling mechanisms of ultra- and microfiltration.

#### *Conclusion:*

*The main foulants have a similar size as the membrane pore size. The fouling mechanism is adsorption or pore blocking.*

*Foulants as organic matters (especially biopolymers) have specific chemical properties which are not yet fully understood (Potts et al. (1981); Cheryan (1988)).*

#### **2.3 Particle behaviour during coagulation, flocculation and micro sieve filtration**

The goal of the coagulation/flocculation is to agglomerate particles to retain them better with a 10 µm sieve. A good way to characterize the process efficiency is to measure the particle size.

### **2.3.1 Effect of coagulation and flocculation**

As seen in the section 2.2, coagulation destabilizes particles by modifying their surface charges. Coagulants with charges opposite those of the suspended solids are added to the water to neutralize the negative charges. Most coagulants are metal salts such as iron (III) chloride  $\text{FeCl}_3$  or polyaluminium chloride PACl. In a process with coagulation and flocculation, these occur in successive steps intended to overcome the forces stabilizing the suspended particles, allowing particle collision and growth of floc. If step one is incomplete, the following step will be unsuccessful. The coagulation with metal salts destabilizes the particle suspension and start the particle agglomeration. The flocculation, a gentle mixing stage, uses polymers to build bridges between the coagulated particles. It increases the particle size from sub-micron flocs to visible suspended particles. Small flocs are formed by chemicals. These large flocs are easier to remove by sedimentation or filtration. The first step (coagulation) is used alone before UF and MF processes. But with a micro sieve filtration, it is essential to create flocs large enough to be retained by the filter ( $> 10 \mu\text{m}$ ). Anionic or cationic polymers can be used, with low or high molecular weight and with low or high surface charge depending on the water quality to be treated.

Finally, particles in water may be present as primary particles, or more often as agglomerates formed from numerous primary particles. These may contain only a few or hundreds of smaller particles attached to each other and held together by interparticle forces. Particle counters do not distinguish between primary particles and aggregate forms (Nieuwenhuijzen A., 2011).

### **2.3.2 Effect of micro sieve filtration: mechanism, fouling**

The filtration in the micro sieve pilot plant is continuous, gravity driven from inside the discs to the outside permeate tank (Langer, 2013). Approximately half of the filter panels submerged to filter the effluent and are progressively fouled, leading to an increase in the water level in the permeate tank. When the high level is reached, the disc filter rotates and the backwash starts cleaning the dirty panels during the continuous filtration of the effluent by the cleaned panels. When the low level is reached, the backwash stops. The backwash is carried out at a pressure of 8 bars with the permeate water.

The micro sieve filter has a pore size of  $10 \mu\text{m}$  which allow all dissolved matter, colloids, and even small particles to pass through the filter. To achieve a good effluent quality, it is necessary to treat the water with coagulation and flocculation before the filtration as explained above. But particles and flocs in water may behave differently when they are exposed to shear flow fields. In the micro sieve pilot plant,  $10 - 30 \text{ m}^3$  of secondary effluent are treated per hour. It means that flocs undergo a velocity gradient of  $10000 - 50000 \text{ s}^{-1}$ . This very high shear force highlights the importance of the coagulation and flocculation processes in the efficiency of the filtration. The flocs which are created have to be strong and stable. Usually, particles with a defined shape are less subject to rupture while Fe- and Al-hydroxide flocs may break apart or are surface eroded under relatively low shear forces. If the hydrodynamic stress is larger than the internal bonding strength, a floc will be disrupted. This may result in poor effluent quality and fouling of the filter by small flocs. Information of floc strength is therefore crucial for the design of floc formation installations with respect to dosing point, placement of pumps, types of pumps, mixing devices and filtration rates (Nieuwenhuijzen A., 2011). One way to characterize the flocs

in the OXERAM project was to use an online particle counter, measuring the particle size in the effluent. The more particles found in the effluent, the less efficient was the coagulation and flocculation processes.

## **Chapter 3 Monitoring of membrane fouling**

### **3.1 Selection of the suitable device**

In the OXERAM project, the specifications of the suitable tool were defined as:

- able to measure particles/colloids in the size range of 1 nm-1µm
- able to measure all types of compounds: inorganics and organics
- able to carry out these measurements in-line or on-line (at least as fast as possible < few minutes)
- able to provide information related to the fouling: size, size distribution, properties, ability to foul membranes
- a tool with a good resolution and reproducibility

Because of their complexity and their size, it has become a great challenge to develop and apply methods for the characterization of organic matter. All methods corresponding to the previous criteria were selected after a literature review) and tested at the TUB at laboratory scale (Boulestreau, 2009).

The advantages and disadvantages of these methods are presented below:

- Microscopic counting: laborious, but exact
- Coulter counter: volume measurements, not suited for particles with low shear strength and below 0.5 µm
- Light scattering with laser beams: rapid method, on-line measurement possible but low reproducibility and reliability
- Laser Induced Background Detector: rapid method, reproducible and reliable but no on-line measurements possible
- Nanosight: rapid, reproducible and reliable, at-line measurements possible

There are currently no methods (non invasive and online) to observe particles in a wastewater treatment process below a lower limit of resolution of 0.5 µm (Chen et al., 2004). After a literature research and after testing various devices, the Nanosight device was selected because it corresponded best to the criteria selected for this project. It does not work on-line but measurements take only a few minutes with a good reproducibility and reliability of the results. Therefore the device can be implemented at-line in a real pilot plant providing data to improve our understanding of membrane fouling. It was recommended to test it directly in the membrane pilot plant.

### **3.2 Materials and methods**

Only the main outcomes are presented in this report, a more detailed version has been written by Schulz (2012).

#### **3.2.1 Nanoparticle tracking analysis: design of device, measuring principle**

##### ***Design of NanoSight NS500***

NTA measurements were performed with a NanoSight NS500 (NanoSight, UK) particle counter for the submicron range. It is equipped with a viewing unit which includes a flow through chamber, a green laser light source (635 nm) and a microscope objective with 20-fold

magnification mounted on a charged-coupled device (CCD) camera, operating at 30 frames per second. Furthermore, the device contains two peristaltic pumps, a sample pump to introduce the sample in the viewing chamber, and a further pump to flush the system or dilute the sample, e.g. with distilled water (see Figure 4). The instrument is controlled by the NTA-Software.

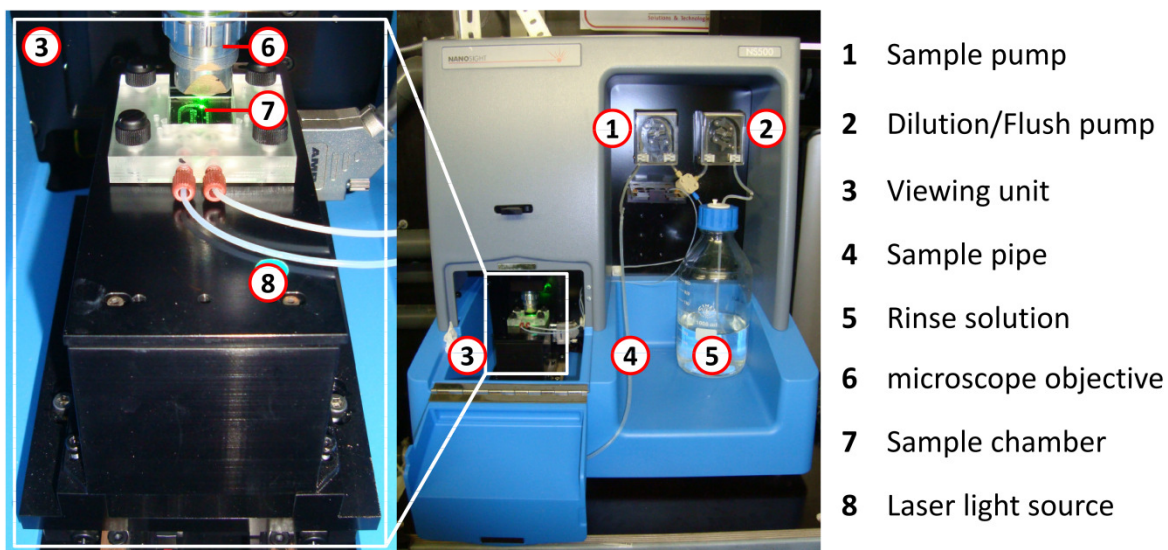


Figure 4: Design of NanoSight NS500 device (right) and the contained viewing unit (left)

#### ***Measuring principle***

The sample is introduced into the viewing unit via the sample pump. The laser beam is passed through a prism-edged optical flat, the refractive index of which is such that the beam refracts at the interface between the flat and a liquid layer placed above it. Due to the refraction, intense illumination region in which colloids present in the liquid film can be visualized via the 20-fold magnification microscope objective (Carr et al., 2009). Colloids in the sample which pass through the beam path appear individually as point-scatters moving under Brownian motion. The camera generates a video of the population of colloids in a field of view of approximately  $100 \mu\text{m} \times 80 \mu\text{m}$  (Figure 5). No calibration of the device or measurement of the refractive index is required.

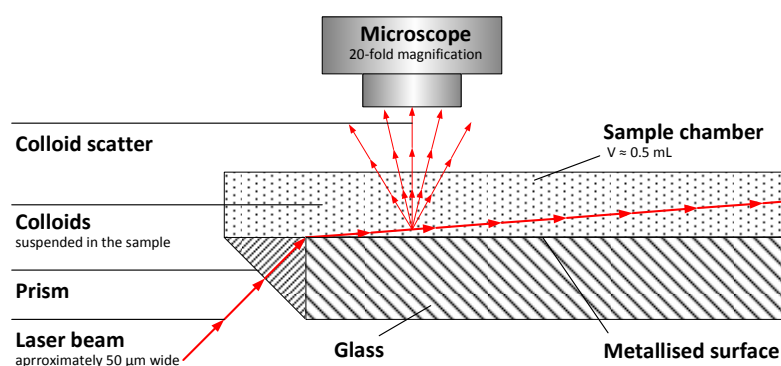


Figure 5: Schematic illustration of the optical path of the laser beam and the detection objective

The NTA-software is then able to analyze the video and to identify and track the centre of each colloid on a frame-by-frame basis throughout the length of the video. The average distances each colloid moves along x and y axes in the image are automatically calculated. From this, the diffusion coefficient  $D_t$  can be obtained and, given the sample temperature  $T$  and solvent viscosity  $\eta$ , the hydrodynamic diameter  $d$  is identified (Stokes-Einstein equation (Carr et al., 2009)). The smaller the colloid, the larger is the distance it moves in a certain time.

#### **Equation 1: Stokes-Einstein equation**

$$\frac{\overline{(x,y)^2}}{4} = D_t = \frac{T k_B}{3\pi\eta d}$$

$D_t$  = diffusion coefficient [ $m^2 s^{-1}$ ]  
 $k_B$  = Boltzmann constant ( $1.380 \times 10^{-23}$ ) [ $J K^{-1}$ ]  
 $d$  = hydrodynamic diameter [m]

Furthermore, the colloid scattering intensity is recorded. The intensity of every colloid is saved in a value compared to the intensity of standard latex particles. In this way a rough assessment of the nature of colloids in the sample is possible.

The range of colloid sizes that can be analyzed by NTA depends on the colloids and the sample type. For colloids with very high refractive indices, such as colloidal gold, accurate determination of size is possible down to 10 nm diameter. For lower refractive index colloids, such as those of biological origin, the smallest detectable size might be between 25 and 35 nm. In highly-concentrated samples with polydispersed mixtures of colloids, tracks of small colloids could be obscured by the noise of larger ones. The upper size limit corresponds to the slowest Brownian motion of a colloid which can be tracked accurately, typically 1 to 2  $\mu m$  diameter (NanoSight, 2010 a+b). To enable a sufficient number of particles to be analyzed within an acceptable time period, samples should contain  $10^7$  -  $10^9$  particles/mL (Filipe et al., 2010).

#### **Video analysis software**

Different settings have to be adjusted in the software before measurement to optimize the quality of the video (Schulz, 2012):

- Dilution of the sample 0 – 100%
- Camera Level: brightness of the image
- Capture duration: 10 – 215 s increase the statistical accuracy
- Focus: determine the acuity of the picture
- Stage: determine the position of the flow through chamber
- Temperature control: a constant temperature can be set
- Viscosity: possibility to set the viscosity of the sample to a fixed value

After the video recording, different settings can be adjusted to optimize the analysis with direct feedback seen on the right side of the screen (Schulz, 2012).

- Detection threshold: qualify an object to be tracked (grey scale)
- Blur: smoothing function to eliminate noise
- Min. track length: min. number of steps tracked by the software to be included in results
- Min. expected particle size: max. search area distance around a colloid between two frames

Standard settings which were used for all further analysis presented in this study are summarized in Table 1.

**Table 1: Standard protocol settings for submicron particles analysis with the NS500 device**

	pre-capturing settings			video analysis settings			
parameter	temperature control	camera level	capture duration	detection threshold	blur size	min track length	min expected particle size
unit	[°C]	[‐]	[sec]	[‐]	[pixel]	[‐]	[nm]
value	25*/off**	16	30*/20**	auto (20)	auto	20	50

\* manual measurement, \*\*online measurement

### 3.2.2 Lab equipment (Genz et al., 2011)

#### Water

The influent water of the pilot plant or of the Jar-Test was the effluent of the WWTP Ruhleben, also called secondary effluent.

#### Ozonation

Pre-ozonation was conducted with an ozonation unit that produces gaseous ozone from pure oxygen using an ozone generator from WEDECO (type Modular 8HC, ITT WEDECO GmbH, Germany). The gaseous ozone provided by the ozone generator was directly introduced into the sample in a 4-L semi-batch stirred tank reactor. An ozone mass balance was set up automatically by a computer as in-gas and off-gas ozone concentration, dissolved ozone and gas flow rate were measured continuously. For completion of the mass balance, the off-gas ozone was completely stripped with pure oxygen. Target ozone dosage was in the range 2-10 mg O<sub>3</sub>/L, corresponding to 0.2-0.9 mg O<sub>3</sub>/mg DOC<sub>0</sub>.

#### Coagulation

Coagulation with FeCl<sub>3</sub> was conducted according to “Technical rule DVGW W 218” (DVGW, 1998) with secondary effluent from WWTP Ruhleben except the volume of the beaker, which was 4 L instead of 2 L. Direct addition of iron (III) chloride into the 4-L-semi-batch stirred tank reactor was followed by a stirring period of 30 seconds at 360 rpm with subsequent stirring at 60 rpm for 5 minutes. Target coagulant dosages were 0-12 mg Fe/L.

#### Amicon cell-Filtration test

Filtration tests were performed according to Zheng et al. (2009) using Amicon filtration cells in dead end mode with the stirrer removed. Each filtration test was started using a new membrane. 100 ml of pure water are filtered through the membrane immediately before the experiment to determine the pure water flux J<sub>0</sub> of the membrane. Flux is recorded with the help of a balance connected to a computer, for each filtration trial only membranes within a 20 % variation of the original pure water flux were applied. For all trials a NADIR® UP150 ultrafiltration (UF) membrane (MICRODYN-NADIR GmbH, Germany) was used. This UF membrane is made of permanently hydrophilized polyether sulphone (PES) and has a molecular weight cut off (MWCO) of 150 kDa. The sample was filled into the feed reservoir and pressurized with a

constant pressure of 1 bar using nitrogen gas. Slow stirring in the feed reservoir prevented the flocs from settling.

#### ***Multi-filtration trials***

Multi-filtration trials were performed to study fouling of differently treated WWTP effluent. The trials were performed as described by Jermann et al. (2007) and above in the section “Filtration tests”. However, filtration experiments were conducted at a constant pressure of 1 bar and with five filtration cycles rather than three. Thus, only the first run was performed with a new membrane. Before each trial, pre-treatment of the membrane and determination of pure water flux of the new membrane were performed as described. During each cycle, 500 mL of permeate were generated. Afterwards the membrane was backwashed using 50 mL of the previously generated permeate at a pressure of 1 bar. Additionally, the flux of the used membrane was again assessed with 100 mL of pure water prior to each filtration cycle.

#### ***Pre-filtration for NTA***

A pre-filtration of the sample for NTA is necessary to remove larger particles. Large particles ( $> 1 \mu\text{m}$ ) could scatter significant amounts of light and mask the presence of smaller particles. Similarly, very large particle aggregates ( $> 10 \mu\text{m}$ ) may affect image quality or might block the sample inlet/outlet ports and should be removed before sample is analyzed. However, the pre-filtration has to be optimized to minimize its impact on concentration and size distribution of colloids  $< 1 \mu\text{m}$ .

A standard protocol for the pre-filtration was defined and kept constant for all analyses, to ensure comparable results. Manual pre-filtration was conducted using  $5 \mu\text{m}$  cellulose nitrate filters (pore diameter = 47 mm) (Whatman®, Germany), fixed in a syringe filter adapter, and a polypropylene syringe ( $V = 60 \text{ mL}$ ). The filter was flushed with 60 mL of distilled water followed by 60 mL of air to remove residual flush water. Afterwards, 60 mL sample was filtered, and the first 30 mL was discarded.

#### ***Analytics***

All analyses to characterize water quality were conducted according to the appropriate German standard methods for the examination of water, waste water and sludge DIN 38402-1:2011-09. Samples of pilot site were measured in the accredited BWB-laboratories (Ruhleben and Jungfernheide, Berlin), either on-site or by online devices. Besides, samples of the lab-scale tests were measured at the laboratories of Department of Water Quality Control, Institute for Environmental Engineering at TU Berlin. Analytical methods and instruments used in this study are summarized in Table 2.

**Table 2: Analytical methods for characterization of water quality**

Parameter	Method according to	Device	Comments
Temperature	DIN 38404 – C04	pH537 Microprocessor* (WTW GmbH, Germany)	-
		Multi 3420 G*** (WTW GmbH, Germany)	Sensor: SenTix 20
pH	DIN 38404 – C05	pH537 Microprocessor* (WTW GmbH, Germany)	-

<b>Turbidity</b>	DIN EN 27027 – C2	Hach 2100N IS * (Hach Lange GmbH, Germany) AL250-IR portable turbidity photometer*** (AQUALYTIC®, Germany) ULTRATURB plus sc online**** (Hach Lange GmbH, Germany)	Ratio-technique (560 nm) 90° - scattered light (infrared) 90° - scattered light (860 nm)
<b>TOC/DOC</b>	DIN EN 1484 – H03***	- Vario TOC CUBE* (Elementar Analysensysteme GmbH, Germany)	Catalyzed-oxidized combustion
<b>LC-OCD</b>	-	LC-OCD analytic system* (DOC-Labor, Dr.Huber, Germany)	
<b>UVA<sub>254/436</sub></b>	DIN 38404 – C03***	- UV-vis spectr. Lambda 12* (Perkin-Elmer, USA)	10 mm quartz cuvette Spurasil
<b>SS</b>	DIN EN 872 (H02)***	-	Filters 0.45 µm: *cellulose nitrate ** glass fibre
<b>COD</b>	DIN EN ISO 11885(E22)**	HachLange LCK 414 (Hach Lange GmbH, Germany)	-
<b>Total aluminium(Al)/ iron (Fe)</b>	DIN EN ISO 11885 (E22)**	-	ICP-OES
<b>Ortho-phosphate</b>	DIN EN 1189	HachLange LCK/ LCS 349*** (Hach Lange GmbH, Germany)	-
<b>Total phosphorus</b>	DIN EN ISO 11885 (E22)**	-	ICP-OES

### 3.2.3 Fouling analysis (see Appendix 2)

### 3.2.4 Pilot plant: online implementation

One of the key objectives of this study was the online implementation of the NS 500 at the membrane pilot unit to monitor the variation of the submicron particle content in the feed water, to investigate the impact of the pre-treatment on it in real-time and to look for a link between colloidal loads and filtration performance of the UF membrane.

#### **Autosampler**

In order to connect the instrument to the pilot plant, an auto-sampling unit was designed with two sample lines, before and after coagulation (Schulz, 2012). Each sample line contains a 5 µm stainless steel pre-filter (cmc-Instruments GmbH, Germany) which removes larger particles. Filters have a cylindrical geometry and are conducted in outside-in mode with an active filter area of 14.7 cm<sup>2</sup>, which is similar to that of the membrane filters. They are mounted in a steel housing (V = 15 mL) containing a feed inlet, a filtrate outlet and an additional feed-side outlet at the bottom of the housing to drain the chamber.

The transport of the sample is carried out by a peristaltic pump (GILSON Minipuls 2, Gilson Inc., UK) with a maximum flow rate of 30 mL/min. It pumps the sample through the system in a flow through cell (FTC) (V = 23 mL) with overflow and drain valve. The NS 500 is connected to the auto-sampler by pumping the sample from the FTC. An additional backwash pump was installed to clean the filters after each filtration with distilled water as well as with acid (5 % H<sub>2</sub>SO<sub>4</sub>). All

parts are connected by PVDF-tubes (Int. diameter = 4 mm, V = 12.5 mL/m) and were fixed on a PVC base plate. The total volume of the system was approximately 60 mL.

All electrical parts (valves, pumps) of the auto-sampling unit are controlled as outputs of a Siemens LOGO! Controller (Siemens AG, Germany). The program of the Siemens controller initiates alternating sampling and flushing of each sample line. One cycle lasts 30 min. The cycle begins with 10 min sampling of SP1, followed by a 5 min flush of the system. During this cleaning process, the FTC is flushed with distilled water, while it is drained four times during the flush period through the valve at the bottom. Furthermore, filter 1 is backwashed starting with 100 sec distilled water flushing, followed by 100 sec sulphuric acid (5 %) and then with 100 sec distilled water again. At the beginning as well as at the end of the flush, the filter housing is drained to remove residual sample/rinse solution. In the following 15 min this procedure is repeated for the second sample line. After 30 min the cycle is finished and starts at the beginning again.

In addition manual maintenance was carried at least twice a week.

#### ***Nanosight script control***

The NS 500 control software contains the possibility to preset a time triggered sequence of several operational commands (script control). As initial step, the command WAITUNTILMIN 15 was chosen, which activates the script after the chosen period, e.g. if set to 15, the program will start the sequence 4 times per hour. This command allows the user to adjust the auto sampler sequences to the Nanosight sequences with time synchronization. The following command is PUMPLOAD and lasts 215 s, replacing the viewing unit volume 2 or 3 times. Afterwards three videos, each 20 sec, are captured of the sample with intermediate short reload. The videos are automatically analyzed with pre-adjusted settings due to the PROCESS command and then deleted to save storage. At the end of the cycle, the system is flushed for 4 min with distilled water, before starting again at the beginning of the script. In this way, 2 measurements with triple-determination are conducted per hour for each sampling point.

#### ***Membrane pilot plant***

Membrane filtration was performed using a ditzer@ XL 1.5 MB 40 W module (Inge GmbH, Germany) including multibore 1.5 hollow fibre membranes. The pore size of this hydrophilized PES membrane is 20 nm (MWCO = 100 kDa). A detailed characterization of the membrane pilot plant is given by Schulz (2012) (3.3.2). The module contained an active membrane area of 40 m<sup>2</sup> and was operated dead-end at constant fluxes from 45, 60 and 75 L m<sup>-2</sup> h<sup>-1</sup>. The module contained two feed-side connection pipes, one on the top and one at the bottom. For filtration, the valve at the bottom was used as feed water inlet. The coagulated feed stream entered the inner side and permeates through the active membrane layer to the outside of the fibres (inside-out 1.5 / 6.0 mm). Backwash of the membrane was time-triggered and conducted at intervals of 30, 45 or 60 min, depending on the operational conditions. However, if a maximum TMP value of 0.8 bar was reached, a backwash was initiated independent of the filtration time. The backwash was performed with permeate by a separate pump, which provided a higher pressure ( $\approx$  3 bar) than the feed-water pump. The backwash-flux was adjusted to 250 L m<sup>-2</sup> h<sup>-1</sup>.

### **3.3 Lab results**

Submicron particle measurement by Nanoparticle Tracking Analysis is a relatively new technique and has rarely been applied, especially in the field of wastewater applications. Only the main outcomes are presented here; a more detailed version is provided by Schulz (2012).

#### **3.3.1 Reproducibility and reliability of the device**

During the first months, extensive work was carried out to develop the method analysis. Experience was gathered with different particles types and sizes. The results of this test phase are presented by Schulz (2012).

Standard particles of various materials (gold, latex, polystyrene, biopolymers) with sizes between 45 and 500 nm were measured separately or mixed in several matrices like distilled water or UF permeate. The video analysis settings were optimized. Solutions of standard particles were diluted to check the particle concentration reliability. Samples were filtered at different filtration volume and mesh sizes. Finally the secondary effluent (highly polydispersed water) was analyzed to test the reproducibility and the operating boundaries of the device.

All tests showed that the absolute values are measurement specific and not comparable to measurements with different boundary conditions or other analytical methods. Keeping that in mind, the reproducibility and reliability of the Nanosight device is good. The limit of detection was 45 nm for inorganic particles like gold and 60 nm with polystyrene standard particles. However, biopolymer compounds were not detected by the device, probably because they react more as organic dissolved compounds and do not scatter light. The limit of quantification was around 100 nm. Below 100 nm the sensitivity of the sensor declines and the distribution curves decreases. In the interpretation, it is important to bear in mind the masking effect of larger particles on smaller particles.

To conclude, the device is well adapted to monitor the variation of the measured parameter which is of interest but not the absolute value of this parameter (e.g. particle concentration for a specific particle size range).

#### **3.3.2 Effect of ozonation and coagulation on effluent water quality**

After the method development phase, the Nanosight device was used to analyze the particle size distribution of the secondary effluent with and without pretreatment. Doses of ozone between 0 and 15 mg O<sub>3</sub>/L (0 – 1.2 mg O<sub>3</sub>/mg DOC<sub>0</sub>) and doses of iron between 0 and 12 mg Fe/L were applied. Experiments were carried out in the lab at the TUB. Results of ozonation trials are presented Figure 6. Results of coagulation trials are presented Figure 7. And results of both ozonation and coagulation are presented Figure 8.

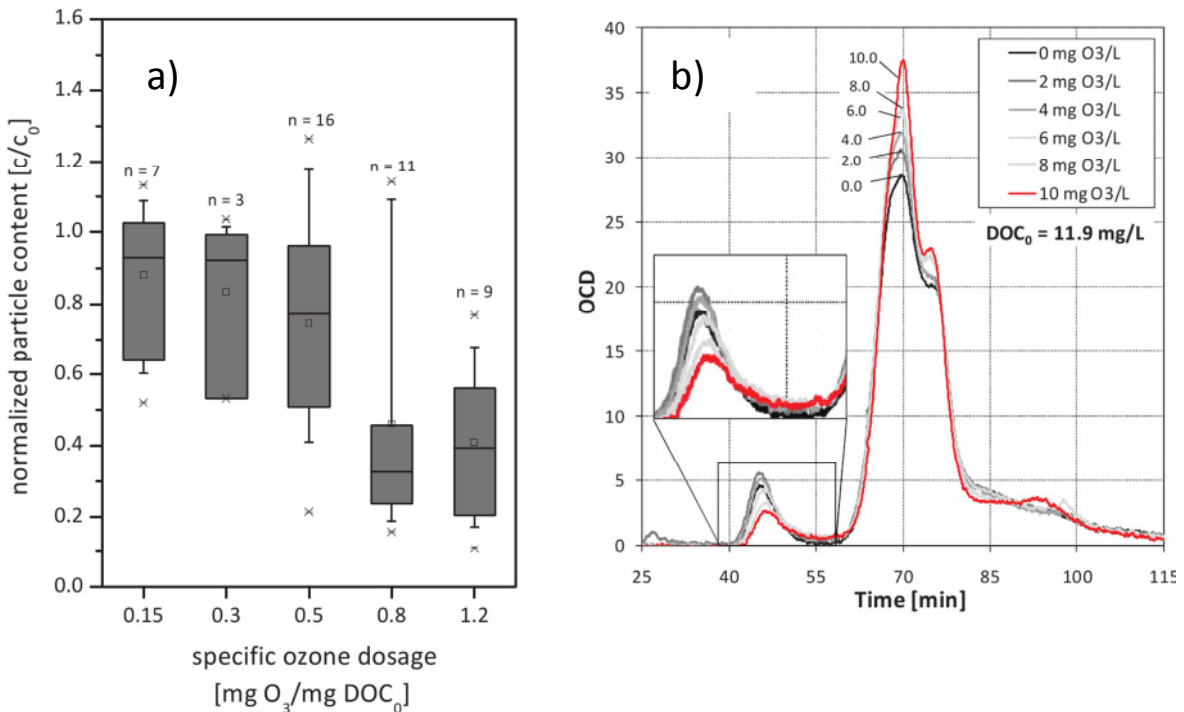


**Figure 6: a) Normalized colloid content (NTA) versus the specific ozone dosage, b) impact of the ozone on the size distribution of colloidal and dissolved organic matter (LCOCM)**

Particle concentrations after ozonation are normalized to the untreated secondary effluent. With increasing ozone doses, decreasing colloid content (50 – 1000 nm) can be detected. At higher doses ( $0.8\text{-}1.2 \text{ mg O}_3/\text{mg DOC}_0$ ), the total particle concentration is reduced by up to 60–80%. We assumed that it is due to a destabilization of the solution and formation of larger agglomerations (Figure 6 a). But even at a dose of  $2.8 \text{ mg O}_3/\text{mg DOC}_0$ , 15–20 % of the colloids was not influenced by the ozonation.

The concentrations of the suspended solids and the dissolved organic matter have also a large impact on the destabilization effect of the pre ozonation, less effective at higher initial SS and  $\text{DOC}_0$  (Schulz, 2012). The ozone consumption due to oxidation competes with the ozone consumption to destabilize the solution.

LCOCM measurements showed a decomposition of biopolymers into smaller compounds like humic substances (Figure 6 b). This shift of high molecular weight compounds into smaller, more hydrophilic fragments confirms the theory described in section 2.2.1. This other effect of ozonation, the decomposition, explains the agglomerating effect. The thickness of the organic coating layer of inorganic colloids is reduced due to this decomposition, which had previously stabilized them via steric hindrance (Jekel, 1986b; Chandranth & Amy, 1996). Hence, microflocculation is induced. Furthermore the higher acidity of the compounds due to ozonation enhances electrostatic interactions between colloids, especially in the presence of alkaline ions, which causes coordinative bonding of functional groups in humic substances, and hence supports agglomeration (Edwards et al., 1994; Becker & O'Melia, 1996). Particle concentration decreases after ozonation due to particles large enough to be removed by the pre filtration or small enough to not be detected by the device.

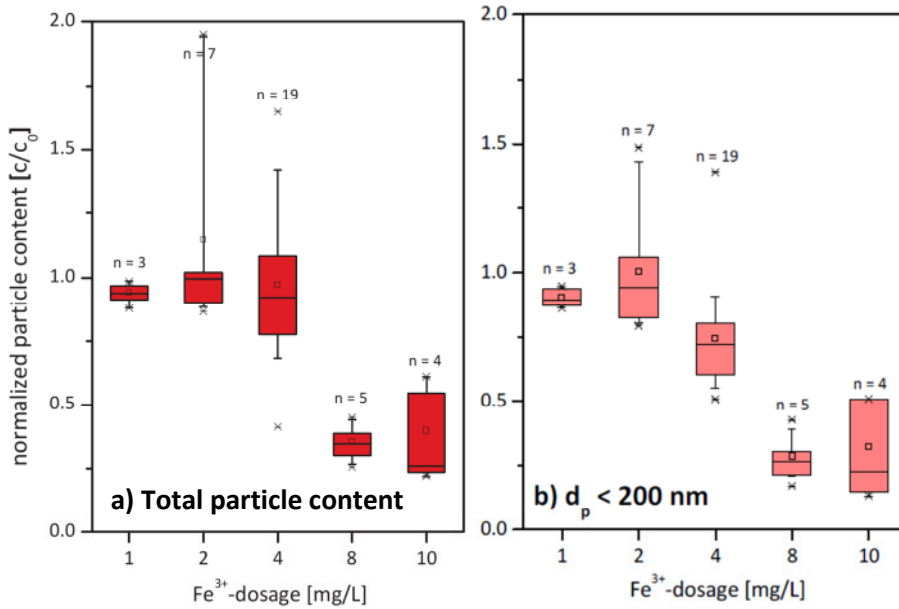


**Figure 7: Normalized colloid content vs. the applied Fe dosage: a) total particle content, b) particle  $< 200 \text{ nm}$**

Increasing Fe dosages lead to decreasing content of submicron particles (Figure 7). A high dose (8-10 mg  $\text{Fe}^{3+}/\text{L}$ ) can reduce the total particle content up to 70-80 % under formation of larger agglomerations. Colloids smaller than 200 nm are preferably removed, as their concentration is decreasing to a larger extent compared to the overall colloid content. But it could also be due to the cake layer formed at higher iron dose. Particularly, high molecular weight fractions, like biopolymers and humic substances are affected by coagulation and are preferentially removed (Haberkamp, 2008; Plume, 2010). Biopolymer removal rates up to 25-30 % with 10 mg  $\text{Fe}^{3+}/\text{L}$  were reached in this study. However, a direct correlation between submicron particle reduction and DOC or biopolymer removal could not be found.

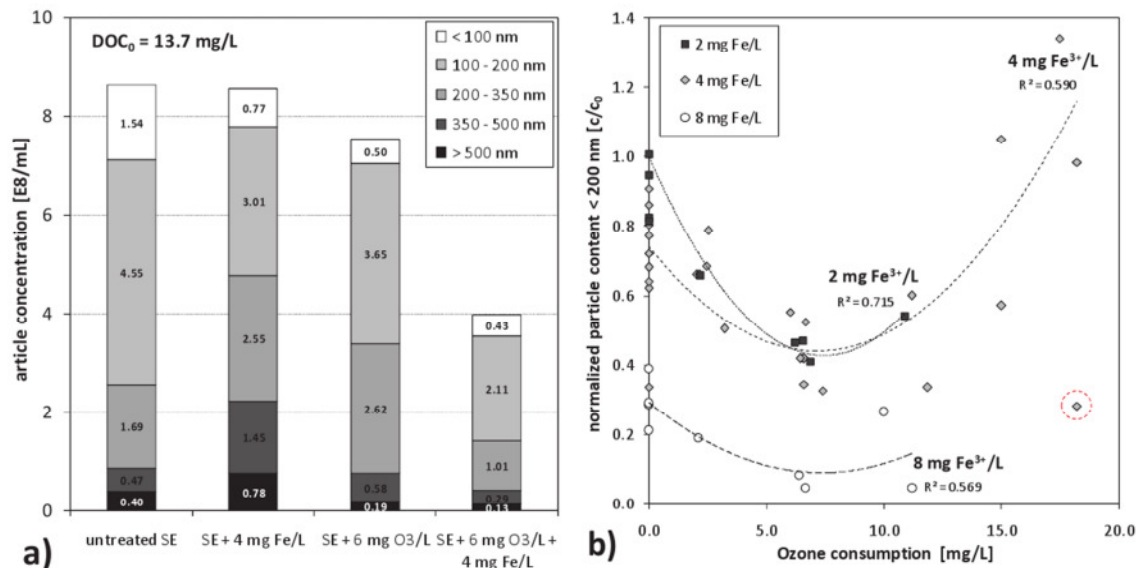


**Figure 8: Impact of pre ozonation and subsequent coagulation on the submicron particle content a) size distribution, b) particle removal  $< 200 \text{ nm}$  at different ozone and coagulant dosages**

Results of an experiment in which samples were treated with 6 mg O<sub>3</sub>/L ( $\approx$  0.45 mg O<sub>3</sub>/mg DOC<sub>0</sub>) without coagulation, 4 mg Fe<sub>3+</sub>/L without pre-ozonation and a combination of both treatments compared to the untreated sample are shown in Figure 8a. The combination of both processes reduces the total particle content by about 50 %. A synergistic effect can be determined as the combined treatments lead to an improved particle removal compared to the effect of the single treatments. An increase in the ozone consumption significantly decreases the content of colloids < 200 nm up to an ozone dosage of 6-8 mg O<sub>3</sub>/L at constant coagulant dosage (Figure 8b). However, above this ozone consumption, an impairment of the effect can be observed at ozone dosages > 10 mg O<sub>3</sub>/L ( $\approx$  0.8 mg O<sub>3</sub>/mg DOC<sub>0</sub>). Based on the results an ozone dosage between 6 and 8 mg O<sub>3</sub>/L ( $\approx$  0.5-0.6 mg O<sub>3</sub>/mg DOC<sub>0</sub>) is recommended for the secondary effluent in Ruhleben. This observation supports the findings of earlier studies, which determine the optimum ozone dosage at 0.1-0.5 mg O<sub>3</sub>/mg DOC<sub>0</sub> (Liu et al., 2009) and 0.1-1.0 mg O<sub>3</sub>/mg DOC<sub>0</sub> (Jekel, 2000). The combination of pre-ozonation and subsequent coagulation offers an opportunity to decrease the necessary usage of coagulants (4 mg Fe/L instead of 8 mg Fe/L), which produces less sludge as well as less solid load on the membrane surface. The combination of the two pre-treatments shows synergy effects and a further colloid removal ranging from 40-80 % can be achieved, depending on the iron dosage. Coagulation becomes more effective with ozonation.

### 3.3.3 Relationship between Nanosight results and Amicon cell filtration performance

In the previous section the Nanosight device analyzed the Ruhleben secondary effluent characteristics as well as the influence of ozonation and coagulation on the water quality in terms of particle size distribution. We now want to study the influence of the water quality on the membrane filtration. Due to the high complexity of the fouling phenomena in low-pressure membrane processes, no universal parameter has been identified to describe the fouling potential of effluent water. By studying both the Nanosight results and the membrane filtration, the goal is to find correlation parameters between organic and inorganic colloids (major foulants) and membrane fouling. The most severe fouling is caused by water constituents with sizes in the range of the membrane pore size, so the colloid size could be one important parameter.

The colloids size impact was investigated at lab scale. For the first trial, the secondary effluent was fractionated at 5, 1, 0.45, 0.2, 0.02 µm. Lab results showed substances between 0.02 - 0.2 µm have the most significant influence on the filterability of the secondary effluent (UP 150, nominal pore size 0.026 µm). In contrast, the largest amount of irreversible fouling is created by the dissolved fraction < 0.02 µm, even though it contributes only to a minor part to the total resistance. In depth investigation of the fouling mechanisms showed that the dominant fouling mechanism with large particles is cake formation. With decreasing pre-filtration pore size, the content of larger compounds in the filtrated water is decreasing which led to a stronger initial pore narrowing/pore blocking behaviour.

In another trial, different sized particle standards (PS 60 nm, PS 200 nm), were added separately and in combination to UF permeate of the pilot plant. Compared to the non-spiked UF permeate, the addition of synthetic nanoparticle standards led to an increase of both total and irreversible fouling resistance in all cases. The strongest increase (> 50 %) in total fouling resistance is induced by the two samples spiked only with 60 nm standard particles.

Trials were performed in which ozone consumptions of 0, 2, 6 and 10 mg O<sub>3</sub>/L were combined with coagulation using 2, 4 and 8 mg Fe<sup>3+</sup>/L. Total fouling resistance of each pre-treated sample is normalized to the total fouling resistance of the untreated sample of the same water and plotted against the ozone consumption at different coagulant dosages (Figure 9a). For each sample filtered by the UF-membrane, the particle size distribution was measured with the NS 500. Figure 9b shows the total fouling resistance in relation to the colloid concentration of different size fractions (50-100, 100-200, 200-350 and > 350 nm) of the samples in one experiment.

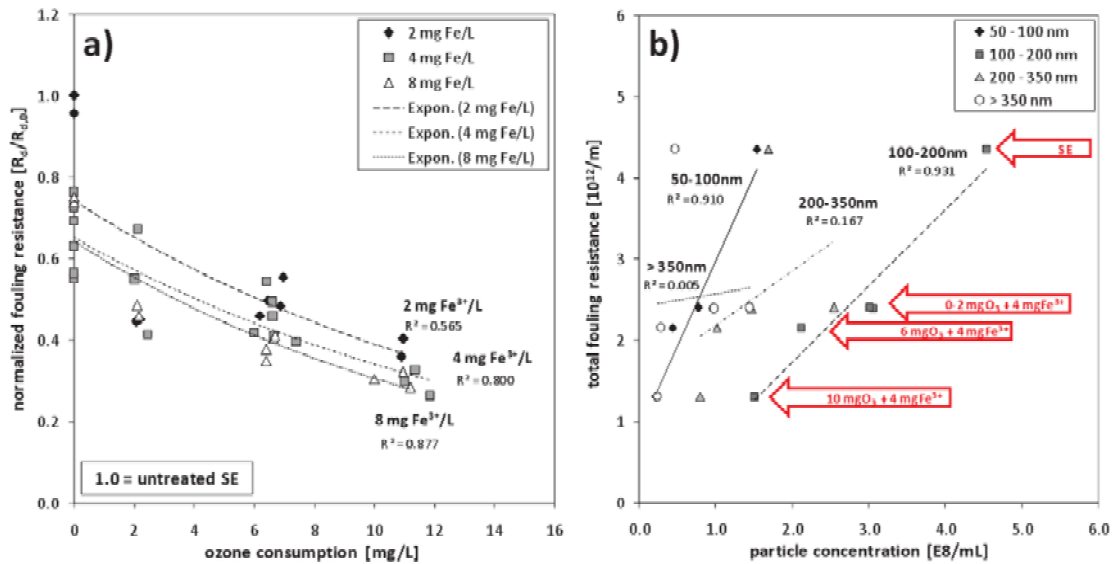


**Figure 9: Impact of pre-ozone and subsequent coagulation on:** a) total fouling resistance normalized to the untreated sample, b) concentration of colloid fractions and corresponding total fouling resistance

Coagulation alone already leads to a decrease of total resistance of about 5 – 35 % depending on the Fe<sup>3+</sup>-dosage. Additional pre-ozone yields a further significant improvement of filterability corresponding to the removal of colloids < 200 nm. Lower dosages of ozone in combination with coagulation reduce the total resistance by about 45 - 65 % whereas an improvement of up to 75 % can be reached by a higher ozone dosage (10 mg O<sub>3</sub>/L). The filtration time for the same sample volume was more than halved due to a pre-treatment with 10 mg O<sub>3</sub>/L combined with 8 mg Fe<sup>3+</sup>/L in two filtration cycles compared to the untreated sample. An increase of coagulant dosage at constant ozone consumption led only to a marginal enhancement of the total hydraulic resistance, which is supposed to be an effect of a higher load of solids and a thicker cake-layer of metal precipitates on the membrane surface. Nevertheless, it is shown that by a combination of both processes, the filtration performance could be significantly enhanced even with low coagulant dosages (Figure 9a).

As shown in Figure 9b, a distinct, linear correlation ( $R^2 > 0.9$ ) can be observed between the content of colloids from 50 to 200 nm and the total fouling resistance. Higher amounts of colloids in this range result in higher total fouling resistances, which confirm that particularly colloids with sizes close to the pores of the membrane tend to block these and lead to a formation of a comparatively dense cake, and therefore cause more severe fouling. Little or no correlation was found for particles above 200 nm. In view of the complexity of the fouling

phenomena, submicron particle analysis by NTA seems to be a promising technique to give a rapid and reliable indication of the filtration behaviour of the water.

The impact of different pre-treatment conditions on the irreversible fouling resistance is shown in Figure 10. Irreversible fouling resistance of each pre-treated sample is normalized referring to the untreated sample of the same water and plotted against the ozone consumption at different coagulant dosages.

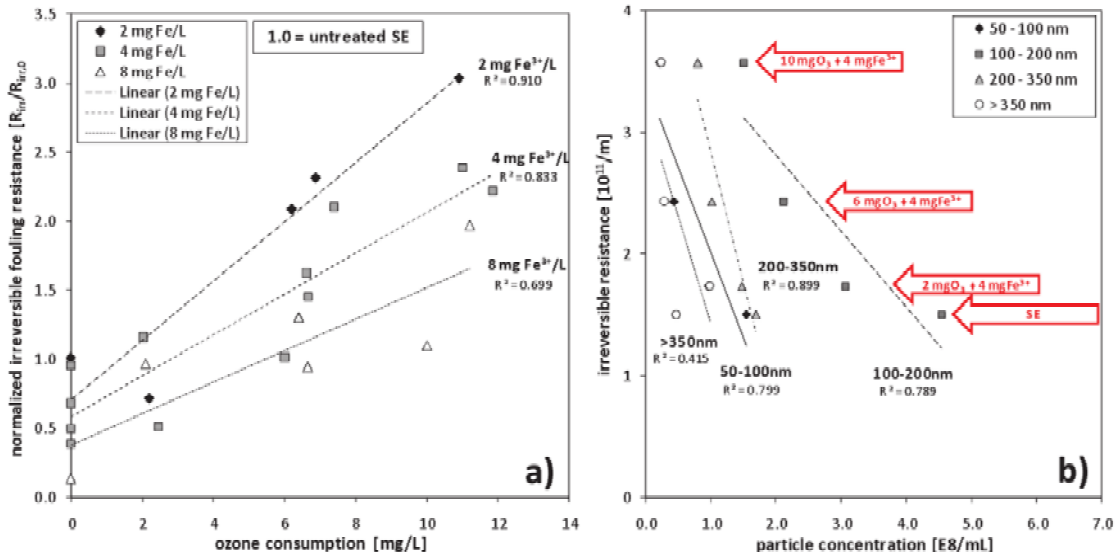


**Figure 10: Impact of pre-ozonation and subsequent coagulation on: a) irreversible fouling resistance normalized to the untreated sample, b) concentration of colloid fractions and corresponding irreversible fouling resistance**

After backwashing the membrane, flux recovery was worse when filtered samples had previously been treated with ozone. The higher the ozone dosage, the more irreversible resistance remains. Coagulation alone decreases the hydraulic irreversible resistance down to 20 % with 8 mg Fe<sup>3+</sup>/L compared to the untreated secondary effluent. Samples treated with additional pre-ozonation show a higher irreversible fouling potential of up to 300 % compared to the untreated secondary effluent. A linear relationship was determined between the applied ozone consumption and the resulting irreversible fouling resistance. Negative impact of ozone is probably caused by a breakdown of large molecules into smaller, more polar fractions which are able to penetrate the membrane pores, adsorb into them and irreversibly foul the membrane (Genz et al., 2011). Another possible reason for the worse behaviour of ozone in combination with this kind of membrane (hydrophilized PES) could be the increasing number of hydrophilic compounds with carbonyl and carboxylic groups due to the oxidation. This hypothesis is promoted by observations during the experiments. The filter cake of coagulated samples could easily be removed by flushing the membrane surface with distilled water, whereas the cake layer on membranes which were filtered with previously ozonated samples was observed to be much tighter and only harder to remove by force. However, coagulation seems to be able to compensate partly for the negative effect of ozone. At constant ozone consumption with increasing iron dosage, the irreversible resistance could be subsequently decreased (Figure 10a). It is suggested that due to the formation of a cake layer of the ferric precipitates, the generated compounds are hindered from penetrating the membrane. This suggestion is confirmed by the

observation that biopolymer rejection decreases with increasing ozone consumption, but can be improved again by an additional subsequent coagulation (results not shown). Nevertheless, to examine the exact origin of the increased fouling by ozonated water, further tests with different pore sizes and membrane materials are required. Furthermore, these lab-scale tests only describe short-term, initial fouling effects. Pilot scale tests are necessary to determine the long term behaviour of this kind of pre-treatment.

Similar to the results of total fouling analysis (Figure 9b), Figure 10b exemplarily presents the irreversible fouling resistance versus the colloid concentration of different size fractions determined in an experiment where the samples analyzed were the untreated and pretreated secondary effluent. The particle concentration seems to decrease with increasing irreversible fouling resistance. The point corresponding to a high particle concentration and a low irreversible fouling is found by analyzing the sample without ozonation. The point corresponding to a low particle concentration and a high irreversible fouling is found by analyzing a sample with highest dosage of ozone. Neither in these experiments nor in further trials could a correlation be observed between the concentration of different colloid fractions and the resulting irreversible resistance. As mentioned, ozonation yields an increase of irreversible fouling irrespective to the particle concentration  $> 50$  nm. The detection limit of the instrument is at 50 nm for that type of water but the nominal pore size of the applied UF-membrane is 26 nm. Therefore, it is not possible to detect water constituents in the size range of the membrane pores. It can be concluded that this method is not able to make reliable estimations of irreversible fouling potential of water filtered through an ultrafiltration membrane, especially when ozone is applied.

### **3.3.4 Determination of effluent composition with scattering intensity measurement (Appendix 3)**

The secondary effluent from Ruhleben contained a broad range of colloid sizes with large variations of scattering intensity (see Figure 34). A very inhomogeneous distribution of intensity rates was observed in the sample, which may indicate the presence of inorganic as well as organic colloids. The bulk of submicron particles have lower intensity rates in the range of latex particles or below, which suggests that they are of organic nature or are coated by dissolved organic substances. However, some submicron particles are found at intensity ranges far above the intensity of polystyrene, which could possibly be of geological origin, like silicates or clays, or residuals of the simultaneous P-precipitation in the biological purification stage.

## **3.4 Online results**

From October 2011 to August 2012, the NS500 was installed at the UF pilot unit. An auto-sampling unit with 5  $\mu\text{m}$  pre-filtration and automated filter cleaning was designed to connect the particle counter to the pilot plant. Semi-continuous sampling and particle measurement of the untreated secondary effluent and the corresponding ozonated and coagulated sample were conducted. Results of the online monitoring and its relationship to the fouling behaviour at the UF pilot unit are presented in this section. Only the main outcomes are presented in this report, a more detailed version has been given by Schulz (2012).

### 3.4.1 Seasonal and daily variations

Colloid concentrations and size distributions in treated domestic wastewaters are wastewater specific and may differ per day or even per hour. Various local factors, like sewer type, landscape, habits, as well as daily conditions, like weather, climate, weekday or daytime, will influence the composition of the colloidal fraction (Nieuwenhuijzen et al., 2003).

Throughout this study, grab samples as well as 24h-mixed samples of the secondary effluent from Ruhleben were taken and analyzed for the submicron particle content, in order to look for the effects of local weather and seasonal conditions. Additionally, online measurements were conducted at the last period of this study. Total particle concentrations and weather data of the gathering ground of WWTP Ruhleben from March to December 2011 are summarized in Figure 11.

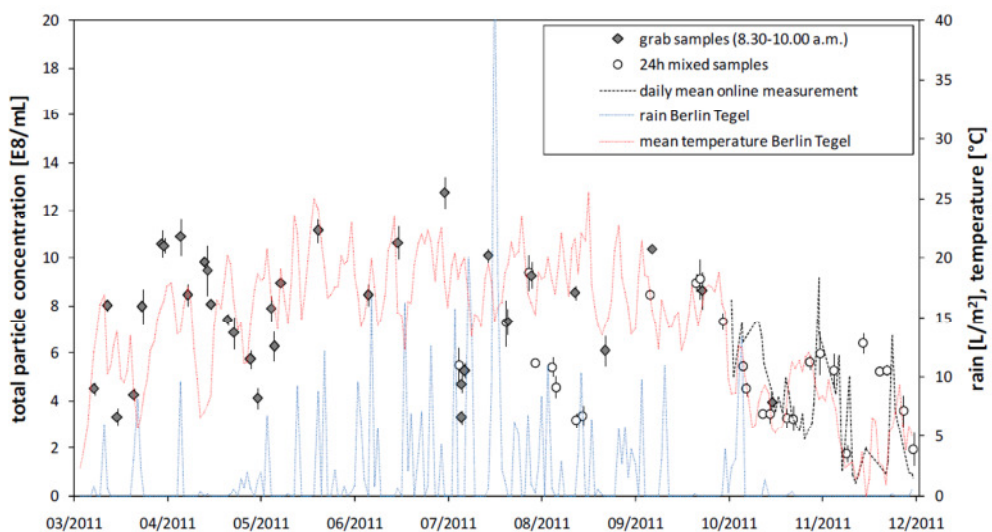


**Figure 11: Variations of submicron particle content in the secondary treated Ruhleben effluent, including grab samples taken between 8.30 a.m. and 10.00 a.m. (n=34), 24h mixed samples (n=27), daily mean values of online measurements (n=42), and weather data for Berlin Tegel during this study ([www.dwd.de](http://www.dwd.de))**

The total particle concentration of secondary Ruhleben effluent shows large variations from  $2.0 - 12.0 \times 10^8$  particles/mL during the period of this study. A clear correlation to seasonal conditions cannot be determined. Nevertheless, a slight trend to lower particle numbers can be detected in colder seasons e.g. at the end of the observational period. Furthermore, longer rain periods led to a decline of particle concentration in the effluent of the WWTP, due to a dilution of the domestic wastewater, as can be seen during some days in July and August in Figure 11. However, colloid concentration depends on numerous other factors and cannot be explained just by seasonal conditions.

The incoming wastewater flow shows strong daily fluctuations, even during dry weather days, due to the varying water demand of households. Figure 12 illustrates the inlet flow of WWTP Ruhleben for six days at the end of October (without rain events), the corresponding total particle concentration (online-measurement NS 500) and the turbidity in the effluent of the plant.

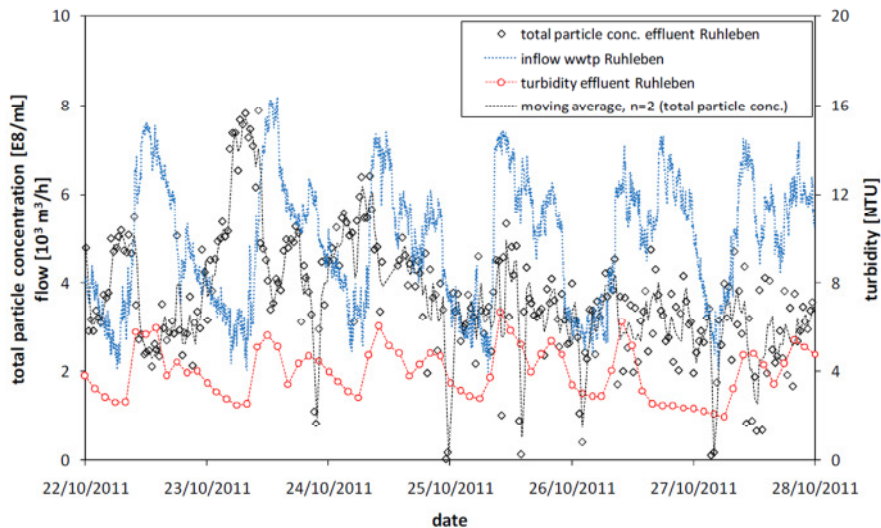


**Figure 12: Daily variation of wastewater inflow to WWTP Ruhleben and corresponding total particle concentration and turbidity in the effluent**

The turbidity in the effluent directly follows the inflow curve of the treatment plant. Peak flows in the inlet lead to a direct increase of turbidity in the effluent water. This trend, which can also be observed for other particle sum-parameters (e.g. suspended solids), can be explained as a consequence of lower retention times of the water in the secondary clarification step. Larger amounts of settleable solids and sludge residuals are able to pass this step and are detected by the turbidity measurement.

The total particle content in the effluent shows different behaviour. The concentration shows the same progression as the inflow curve of the treatment plant, but with a delay of 18-20 hours. The submicron particles seem not to be effectively retained by the classical treatment steps and, therefore higher loads in the influent stream lead to a higher charge in the effluent (after 18-20 h). This period represents the time which is necessary for a certain water volume to pass the whole treatment process. The steady decrease in the detected particle concentration may be the result of clogging effects on the 5 µm pre-filter.

High loads of submicron particles are emitted during the peak periods of wastewater volume in the morning and in the afternoon. This content, therefore, seems to originate from households/human sources or to be washed out of the sewer system due to higher flow rates during these periods. No correlation of total particle content could be found to particle sum parameters like turbidity or suspended solids. Colloid concentration is not affected by the flow velocity during clarification steps, as they are not settleable. Retention of submicron particles by co-settling during the clarification steps, as described by other researchers, only seems to play a minor role (Wu & He, 2010).

It can be concluded that large daily variations can be observed in colloid concentrations of the effluent of WWTP Ruhleben. Although a slight dependence on seasonal conditions is apparent, daily circumstances have the largest impact on submicron particle content in the secondary effluent. A high resolution measurement is necessary to detect these variations. Nevertheless, the applied online measurement system is able to provide reliable determination even of slight variations.

### 3.4.2 Effect of coagulation on effluent water quality

#### 3.4.2.1 Inline coagulation: impact of coagulant dose and type

The removal of colloids < 200 nm by in-line coagulation at the UF-pilot unit detected by online measurements with the NS 500 is illustrated in Figure 13. It shows the progression of the colloid content < 200 nm in the UF-pilot inlet and after coagulation with 4 mg Fe<sup>3+</sup>/L during three days in October 2011. The colloid concentration after coagulation follows strong daily fluctuations and critically depends on initial colloid concentration of the secondary effluent (Figure 13a). When more colloids < 200 nm are present in the inlet of the pilot plant, more colloids can be detected after coagulation and are able to reach the membrane surface. However, peak concentrations can be compensated partly by coagulation, which for example was observed on the evening of October 21 and during the night of October 23.

Because of these strong variations in the feed water, the colloid removal rates detected by the online measurements also show larger fluctuations compared to the lab-scale tests. A median removal with 4 mg Fe<sup>3+</sup>/L (0.072 mmol Fe<sup>3+</sup>/L) accounted for 50-60 % by in-line coagulation (Figure 13b), whereas at lab scale, an average removal of around 30 % was obtained at the similar coagulant dosage (Figure 7b). However, the lab and online pre-filters have different properties; therefore a direct comparison has to be made with caution and is only possible to a limited extent.

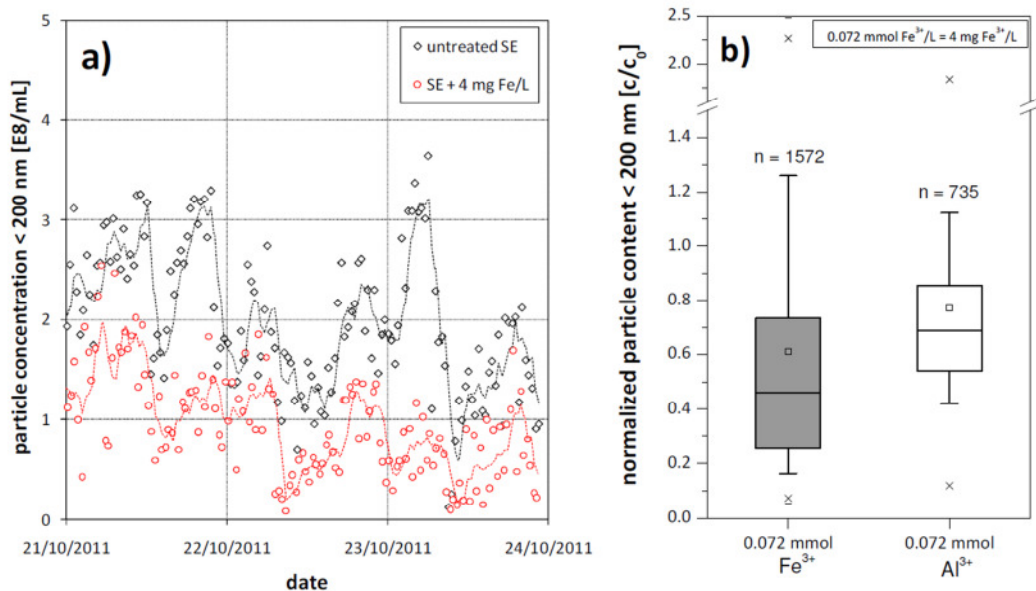


**Figure 13: Colloid removal (< 200 nm) by coagulation in the UF-pilot unit: a) Behaviour of colloid removal in dependence to initial concentration, b) comparison of removal by different coagulants (FeCl<sub>3</sub>, PACl)**

Iron (III) chloride (FeCl<sub>3</sub>) as well as polyaluminum chloride (PACl) were tested as a pre-treatment for the UF pilot unit at the WWTP Ruhleben during this study. At similar dosages (here 0.072 mmol/L) and constant operational conditions, better colloid removal was observed with FeCl<sub>3</sub> as coagulant ( $\approx$  55 %) than for PACl ( $\approx$  30- 40%) (Figure 13b). This is possibly due to the water pH. Both coagulants have an optimum pH value, namely 6.5 – 9.0 for Fe and 6.0 – 7.0 for Al, in which the insoluble neutral species (Me(OH)<sub>3</sub>) are dominating and will precipitate (Jekel, 2004). The pH of the secondary effluent ( $7.4 \pm 0.2$ ) is slightly above the optimum pH for PACl and therefore

precipitation may be incomplete and less colloids removed. However, differences could be also due to a changing water quality between the experimental phases.

Figure 14 shows the filtration behaviour of feed-water treated with 4, 8 and 12 mg Fe<sup>3+</sup>/L, at the UF-pilot unit. Each pre-treatment was applied for 12-14 days while other operation conditions were kept constant to achieve comparability. Operating flux was 60 L m<sup>-2</sup> h<sup>-1</sup> at a filtration time of 60 minutes between permeate backwash of 35 s. Once a day, a chemically enhanced backwash was carried out (steps in each curve). Starting permeability after each backwash is referred to the initial value and normalized to 20 °C.

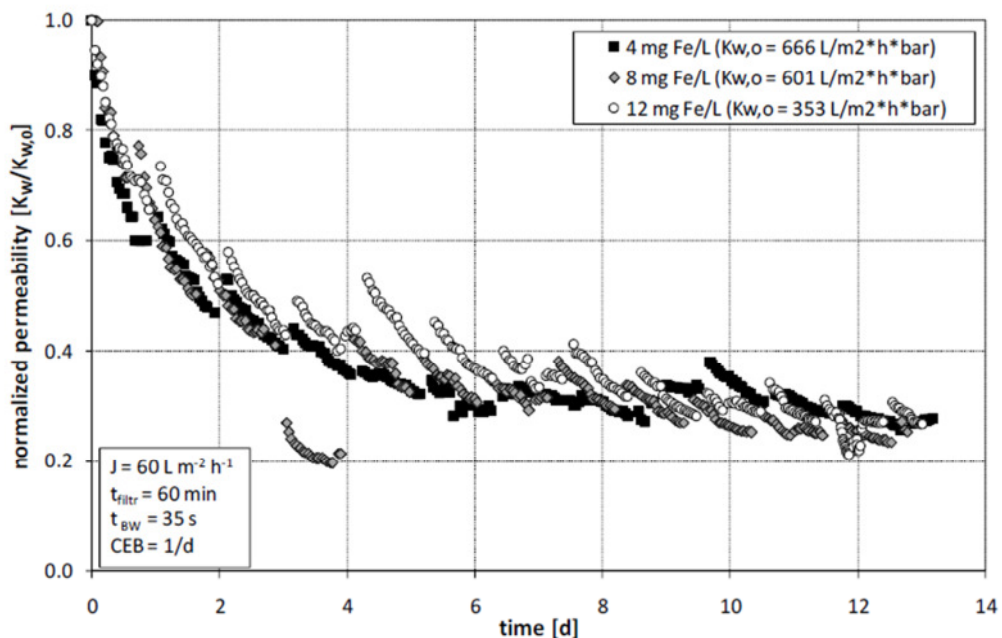


**Figure 14: Development of the normalized starting permeability after each backwash of the UF-pilot unit at trials with three different coagulant dosages between 17 October and 1 December 2011**

Similar to the lab-scale findings, it was observed that due to an increasing coagulant dosage the reversible fouling behaviour of the water is only slightly improved because coagulation increases the solid load in the membrane fibres and on the membrane surface (results not shown). However, with increasing coagulant dosage the irreversible fouling could be reduced particularly during the first 8 days of the trials. This is indicated by higher permeability values after each backwash, especially with 12 mg Fe<sup>3+</sup>/L, Figure 14. Higher coagulant dosages mean that the TMP can be lower corresponding to a higher permeability. Furthermore, the effectiveness of the applied CEBs was enhanced at higher coagulant dosages, which lead to higher steps of the start permeability after each CEB. This matches with a removal of submicron particles observed at lab-scale and a formation of more porous cake by larger agglomerates due to coagulation, which hinders foulants from penetrating the membrane pores and adsorbing into them. Nevertheless, after 12-13 days all curves were reaching a similar value of 20-30 % of the initial permeability. A multitude of factors impact the filtration performance of the membrane and partly lead to a lack of comparability of those trials. Besides water quality, which naturally shows strong daily but also seasonal variations, operational conditions, e.g. applied flux and filtration time, significantly affect the fouling behaviour. Furthermore, although CIPs were carried out before each experimental trial, the membrane module is still affected by previous experiments and

cleaning efficacy therefore varies significantly, even when the same cleaning conditions are applied. Furthermore, a fouling prediction of the water by detecting specific constituents can never be fully representative. However, it can serve as a good indicator for assessing the water fouling potential.

### 3.4.3 Relationship between submicron particles and filtration behaviour

Figure 15 illustrates the course of particle content  $< 200$  nm after a pre-treatment by coagulation with  $1.9$  mg Al<sup>3+</sup>/L and the corresponding total fouling resistance of the UF membrane, each between two backwashes during three days in October 2011. It can be seen that the total fouling resistance of each filtration cycle is significantly impacted by the concentration of the submicron particles  $< 200$  nm in the water, detected online by the NS500. Colloid peaks in the feed stream led to an increase of TMP and total fouling resistance, whereas lower colloid amounts result in a less steep increase of the TMP. The online measurements validate the good correlation between colloid concentration  $< 200$  nm and membrane performance, which was found at lab-scale.

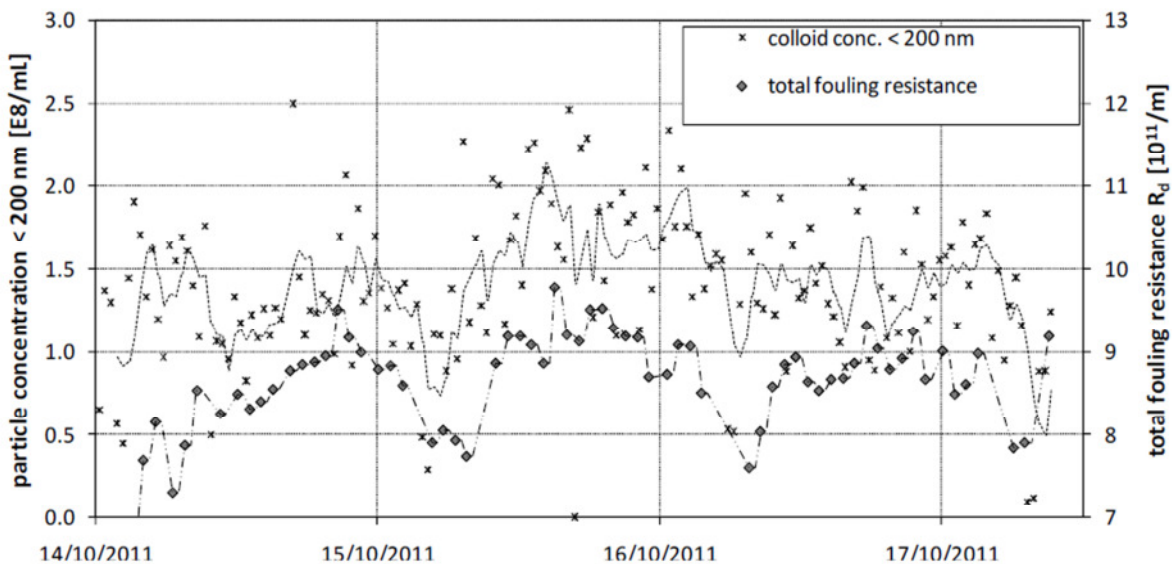


**Figure 15: Development of total fouling resistance per filtration cycle and corresponding online measured concentration of colloidal fraction ( $< 200$  nm) of coagulated secondary effluent (1.9 mg Al<sup>3+</sup>/L)**

The relationship between certain colloidal fractions after coagulation by  $1.9$  mg Al<sup>3+</sup>/L and the resulting total and irreversible fouling resistances per filtration cycle in the UF pilot plant of the experimental trial is shown in Figure 16. As also observed at lab-scale, the filterability of the water is most reliably represented by the content of colloids  $< 200$  nm, as it shows the best correlation to the total fouling resistance ( $R_2 = 0.42$ ). However, the correlation is less significant compared to the experiments under laboratory conditions. The operational conditions and cleaning efficiency as well as the condition of the membrane surface and the membrane module have a large impact on the filtration performance. In the test cell experiments an unused membrane was used for each trial, whereas at pilot-scale aging effects of the membrane or blocked hollow fibres can lead to increasing filtration resistance independently from water quality. Therefore, not all fouling effects can be explained just by foulant loads in the feed water.

Nevertheless, regarding the water quality, the submicron particle measurement seems to be an adequate method for a rapid assessment of the total fouling potential.

In contrast, a relation between any fraction of submicron particles and the short term irreversible fouling resistance could not be determined (Figure 16b). This confirms the observations of the lab-scale experiments. As the device is not able to detect smallest colloids ( $< 50 \text{ nm}$ ) and dissolved foulants, which are known to have a large impact on the irreversible portion of fouling, a reliable prediction of the irreversible fouling potential is not possible using this device.

Figure 16c summarizes the relation between different sized colloids load between two CEBs and the corresponding long-term irreversible fouling, including all experimental trials which were monitored by an online measurement during this study (pre-treatments: 4, 8, 12 mg  $\text{Fe}^{3+}/\text{L}$ ; 1.9 mg  $\text{Al}^{3+}/\text{L}$ ).

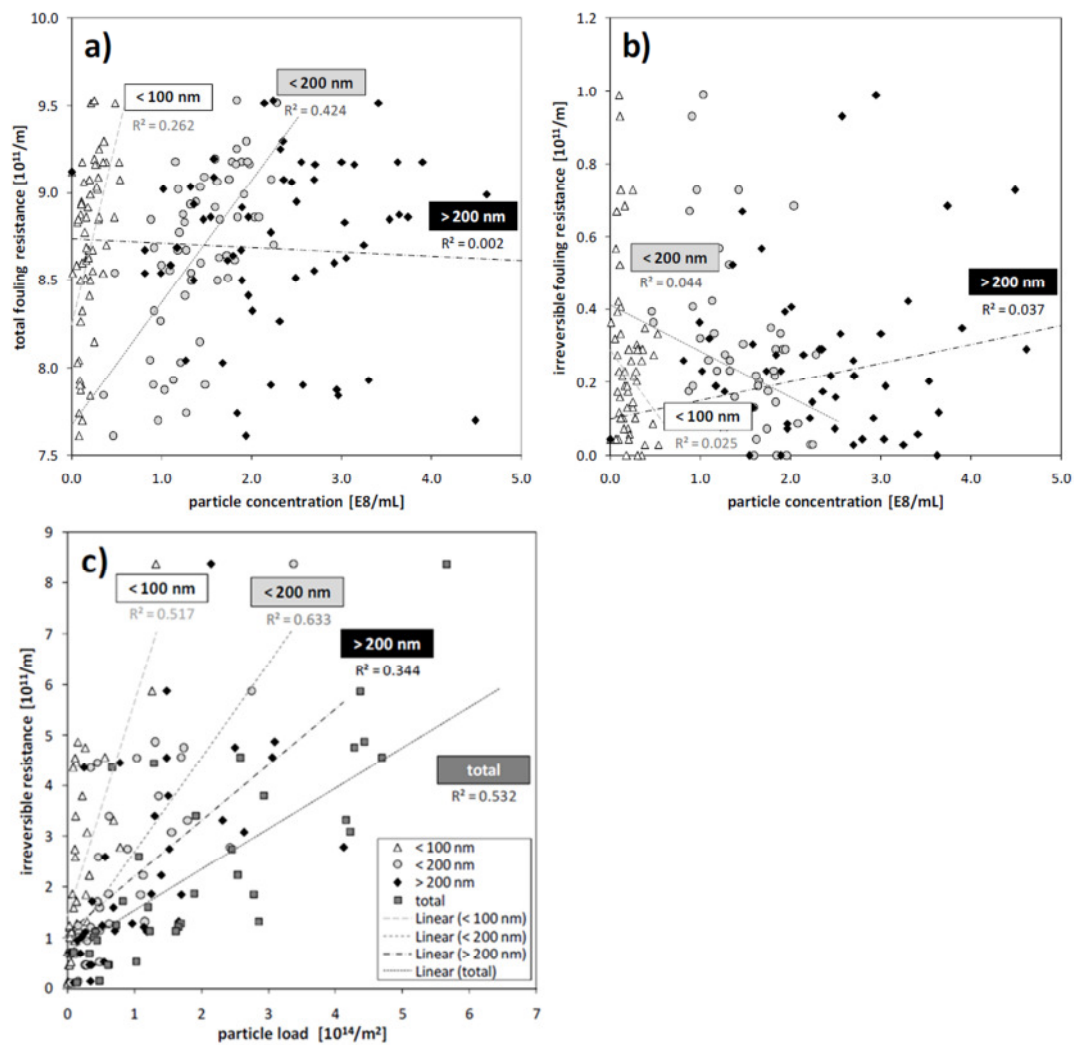


**Figure 16:** Relationship between colloid concentration of different fractions after coagulation by 1.9 mg  $\text{Al}^{3+}/\text{L}$  and a) total fouling resistance, b) irreversible fouling resistance, c) relationship between particle load and long term irreversible fouling during a UF-filtration trial

Concerning long-term hydraulic irreversible fouling, the colloidal load on the membrane can serve as an indicator, even if no direct correlation could be found between the actual deposit colloid amount and the TMP recovery. In periods with larger amounts of submicron particles in

the water, a higher increase of irreversible fouling between two CEB could be observed. The best correlation again was found for the small colloid fraction < 200 nm. Although different water constituents contribute to irreversible fouling, these observations reflect the small colloidal fraction relevance with respect to irreversible fouling resistance during low-pressure membrane filtration.

### 3.5 Comparing Nanosight results with other parameters

Only the main outcomes will be presented in this report, a more detailed version has been presented by Schulz (2012).

#### 3.5.1 Submicron particles and other analytical parameters

Results of correlation analysis of selected parameters are presented in Table 3, where n represents the number of corresponding samples, and R the Pearson correlation coefficient, which is sensitive to a linear relationship between two of the variables. The entire correlation matrix is given in Appendix B (Figure B.1a+b; Schulz, 2012). Absolute R values above 0.5 are considered to be significant.

No correlation of submicron particle content was found with organic sum parameters like DOC, UVA<sub>254</sub> or COD, or for ferric and total phosphorus content. A weak negative correlation appears with the contents of suspended solids (SS) in the water, which increases with increasing colloid size. This underlines the different behaviour of larger particles and submicron colloids. Furthermore, it cannot be excluded that the thicker filter cake during the pre-filtration of the sample leads to a higher retention of submicron particles when higher amounts of larger particles (SS) are present. A similar slight negative correlation is obtained between turbidity and smaller colloid fractions (< 400 nm), whereas a positive dependence was found with larger particle fractions (> 400 nm). This could be explained by the fact that larger colloids are better detectable by turbidity measurements.

**Table 3: Selected results of the correlation analysis (R = Pearson correlation coefficient; p = 0.05)**

Colloid conc.		DOC	UVA <sub>254</sub>	COD	SS	turb.	Fe	P <sub>t</sub>	BP-OC	C/N
Total	R	0.082	0.174	-0.033	-0.315	-0.290	-0.259	-0.291	0.108	0.515*
	n	25	25	25	25	11	24	25	22	22
< 200 nm	R	0.095	0.120	-0.060	-0.244	-0.311	-0.214	-0.271	-0.025	0.522*
	n	25	25	25	25	11	24	25	22	22
200 - 300 nm	R	-0.105	0.185	-0.048	-0.337	-0.302	-0.277	-0.271	0.119	0.415
	n	25	25	25	25	11	24	25	22	22
300 - 400 nm	R	0.126	0.322	-0.028	-	-0.302	-0.331	-	0.200	0.383
	n	25	25	25	25	11	24	25	22	22
> 400 nm	R	-0.091	-0.016	0.215	-0.108	0.489	-0.020	-0.167	0.438*	0.190
	n	25	25	25	25	11	24	25	22	22

\* significant correlation

Between biopolymers and the colloid content < 400 nm no correlation can be observed, which confirms that the magnitude of these macromolecules are not responsive for this kind of optical measurement. A significant correlation seems to exist between larger colloids (> 400 nm) and the biopolymer content. However, this behaviour cannot be fully clarified in this context. A significant relation between small colloids (< 200 nm) and the ratio of C/N occurs, probably due to larger organic colloids like extracellular organic matter originating from the biological treatment. Further investigations are necessary to confirm this suggestion.

In conclusion, it can be noted that most of the correlated parameters show little or no correlation to several fractions of submicron colloids. Especially the small colloids (< 200 nm), which are believed to have the largest impact on low-pressure membrane fouling, are not represented by other water quality parameters. Therefore analyses by NTA could be a promising improvement in furthering the understanding of this effect.

### **3.5.2 Dissolved organic carbon (DOC)**

Coagulation lowers the content of dissolved and colloidal organic substances. Removal rates range from 3-5 % of the DOC with 2 mg Fe<sup>3+</sup>/L up to 10-12 % with 10 mg Fe<sup>3+</sup>/L. Particularly, high molecular weight fractions, like biopolymers and humic substances, are affected by coagulation and are better removed (Haberkamp, 2008; Plume, 2010). Biopolymer removal rates up to 25-30 % with 10 mg Fe<sup>3+</sup>/L were reached in this study. However, a direct correlation between submicron particle reduction and DOC or biopolymer removal could not be found. A slightly positive correlation was observed between the initial  $DOC_0$  and the particle removal (results not shown). The higher the content of dissolved organic substances, the more submicron particles were removed. This effect could be explained by formation of bigger, more voluminous precipitates if a higher DOC content is present, which may lead to a higher amount of removed colloids by sweep coagulation. The effect of the pH shift is negligible. It can be concluded that the removal of submicron particles by coagulation is not directly dependent on any other analyzed parameters. A reliable prediction of the removal potential for colloids by coagulation is not possible.

### **3.5.3 Liquid Chromatography - Organic Carbon Detection (LC-OCD)**

The LC-OCD technique characterizes dissolved organic matter (DOM) in samples filtered at 0.45 µm. The size-exclusion chromatography separates the DOM in several fractions, larger organic compounds elute in the liquid phase faster than smaller ones. Coupled with an organic carbon detector, a UV-detector at 254nm (UVD) and an organic nitrogen detector (OND), these fractions can be analyzed. Table 4 presents the organic substances analyzed as well as their elution time, their size and their properties.

**Table 4: Organic substances size and weight distribution (modified after Crittenden et al., 2005, Filloux, 2006, Hofmann & Kammer, 2009)**

Fractions	Elution time in LC-OCD (min)	Size	Properties
Biopolymers	30 < t < 45	> 10 kDa	High molecular weight compounds (>10 kDa), typically polysaccharides and proteins
Humic substances	45 < t < 59	1 – 20 kDa	(1-10 kDa), mainly fulvic acids (90%) and humic acids
Building blocks	55 < t < 59	350-500 Da	Degradation result of humic acids

LMW acids	59 < t < 66	< 350 Da	Carboxylic acids, alcohols aldehydes, ketones, amino acids (ionic form)
LMW neutrals	66 < t < 250	< 350 Da	id (neutral-form) and aromatic compounds

According to the MWCO, the equivalent pore diameter (in nm) can be approximated by using the equation (Filloux, 2006, after Crittenden et al., 2005).

$$d = 0.11 \times M^{0.46}$$

Where  $d$  is the hydrodynamic diameter of the standard dextran molecule (nm) and  $M$ , the molecular weight according to MWCO (g/mol).

It means that only humic substances and biopolymers are large enough to be a membrane foulant (UF or MF). Other compounds pass through the membrane without being affected.

The same samples were analyzed by the LC-OCD at the TUB and by the Nanosight device operated by the KWB at the Ruhleben WWTP from Mai 2011 to Mai 2012. The objective was to find a correlation between results to better identify which kind of compounds are the most responsible for the fouling in term of size (Nanosight) and nature (LC-OCD).

The higher the R absolute value, the stronger is the correlation studied. In this study we considered all absolute values above 0.5 as representative of a good correlation.

**Table 5: Correlation between LC-OCD and Nanosight results**

R	50< <100nm	100< <200nm	200< <300nm	300< <400nm	400< <500nm
<b>Bypass</b>	0.317	0.660	0.652	0.595	0.477
<b>Chromatogram</b>	-0.357	0.102	0.019	0.005	-0.263
<b>Biopolymers</b>	0.586	<b>0.809</b>	<b>0.782</b>	<b>0.718</b>	<b>0.676</b>
<b>Humic substances</b>	-0.575	-0.208	-0.307	-0.322	-0.518
<b>Rest</b>	-0.289	0.129	0.077	0.085	-0.199
<b>UV</b>	<b>0.874</b>	<b>0.613</b>	<b>0.595</b>	<b>0.390</b>	0.653
<b>TN</b>	0.143	<b>0.480</b>	0.368	0.391	0.296
<b>C/N</b>	0.138	-0.139	-0.048	-0.146	-0.047

The BP was the parameter which presented the strongest correlation with Nanosight results. All other LC-OCD parameters presented a low correlation with the Nanosight size ranges which shows the limitation to use both these devices together to identify the size and the nature of the membrane foulants. Further research needs to be done in this domain.

### 3.6 Operational experiences

During this study, it was possible for the first time to measure online (every 15 min) submicron particles concentration in a secondary effluent. It provided much data to help the operator to understand the membrane fouling phenomena. However this combined system (autosampler + NS500 device) needs optimization. The maintenance work load was high (around 11 hours per week). This was due to small tube clogging or filters clogging which needed regularly cleaning either with distilled water or with chemical products such as acid or sodium hypochlorite. More efficient or automatic system could be built to ease the operator work. It also has a high impact on the quality of results as the clogging of the pre-filter directly influences the particle removal above 1 µm before the measurement. Automatic daily pre filter cleaning could reduce the impact of the cake layer formation on the Nanosight results. The filter cleaning has to include high pressure backwash and a chemically enhanced cleaning step in order to avoid long term clogging effects and negative influences on the measurement.

### **3.7 Conclusion on online monitoring of membrane fouling**

In this study the fouling behaviour of treated domestic wastewater during low-pressure membrane filtration was investigated by sizing and counting the submicron constituents using Nanoparticle Tracking Analysis (NTA). The goal was to find a link between colloidal loads and filtration performance. A pre-treatment by ozonation and/or coagulation had to be optimized in order to improve the removal of fouling-active colloid fractions and to achieve the best possible prevention of membrane fouling. An online installation of the instrument was conducted to investigate its potential for real-time prediction of the water fouling behaviour and possible ways of adapting the pre-treatment conditions. Particle analysis by NTA was obtained to give reliable and reproducible information about the concentration and size distributions of the colloidal fraction in the tested treated domestic wastewater.

A consistent detection of variations in colloid concentration can be carried out in a range between  $1 \times 10^8$  and  $2 \times 10^9$  particles/mL even in organic-rich matrices. In investigations with particle standards, the limit of quantification of NTA was found to be between 45 and 60 nm. For secondary effluent samples, the range for absolute quantification was observed between 100 and 1000 nm. Between 50 and 100 nm not all colloids are detected due to a loss of sensitivity of the measurement (only relative comparison). Below 50 nm the detection is not possible (especially of organic/organic coated colloids like biopolymers). This indicates that especially for UF membranes (pore diameter  $\approx 10 - 100$  nm) some small foulants which are able to block or enter the membrane pores cannot be detected by NTA. Further testing could investigate the option of "marking" smaller colloids to increase their scattering intensity in order to decrease the limit of detection of the device.

A general observation is that the detected particle concentration as well as the quantification of single size fractions largely depends on the polydispersity of the sample and the configuration of the video analysis. Absolute values detected by NTA are measurement specific and not comparable to measurements with different boundary conditions or other analytical methods.

A key step during submicron particle analysis is the pre-conditioning of the sample. It has a large impact on the colloid concentration and size distribution in the sample. For the purpose of minimizing errors and reaching comparable results, prefiltration has to be done under defined conditions with the smallest possible filtration volume. For manual measurements, other options for sample pre-conditioning (centrifuging, settling) should be studied in further investigations to exclude effects of the filter cake on the colloid measurement. For online measurements, the focus should be put on the optimization of automated sampling.

The secondary Ruhleben effluent contains a typical size distribution which increases exponentially with decreasing particle size up to the device detection limit (100 nm for the NTA method). Total particle concentrations of the secondary Ruhleben effluent show large variations from  $2.0 - 12.0 \times 10^8$  particles/mL during the period of this study. A clear correlation to seasonal conditions could not be determined. However, due to the online installation and the resulting more highly resolved measurement, it could be demonstrated that submicron particle concentrations in the secondary effluent are largely dependent on the daily flow curve of the WWTP. It was concluded that colloid fractions, which are believed to have the largest impact on low pressure membrane fouling, cannot be described by classical particle sum parameters like turbidity or suspended solids or by other water quality parameters. Therefore, its analyses by NTA could be a promising improvement in furthering the understanding of the fouling

phenomenon. Moreover, an analysis of the intensity data recorded during Nanoparticle Tracking Analysis should be further investigated. It could give more detailed information about the composition and nature of colloidal fraction of the water as well as on differences in the impact of the pre-treatments.

Ozonation as well as coagulation was found to be an appropriate treatment to reduce the content of small colloids < 200 nm by forming larger agglomerates. It was demonstrated that contents of dissolved organic matter as well as of suspended matter have a significant impact on the removal efficiency during ozonation (Schulz, 2012). In contrast to the observed microflocculation of colloids, the dissolved organic compounds were observed to be decomposed by ozone forming smaller, more hydrophilic fragments which could be detected by size exclusion chromatography. With coagulation alone, small fractions < 200 nm (compared to large fractions) are preferentially removed and a shift of the size distribution to larger fractions occurs. Online measurements at the pilot-scale confirmed these results, indicating that colloid peak concentrations can be compensated for by coagulation. Furthermore, a comparison of  $\text{FeCl}_3$  and  $\text{PACl}$  demonstrated that the former is more effective in colloid removal in this treated domestic wastewater, which matches observations of its higher potential for fouling prevention in earlier studies. Due to the combination of pre-ozonation and subsequent coagulation, a synergy effect was determined as the combined treatments lead to a better particle removal compared to the effect of the single treatments with the same dosages of  $\text{O}_3$  and  $\text{Fe}^{3+}$ . The best results concerning colloid destabilization in the secondary Ruhleben effluent were obtained at specific ozone dosages of 0.5 - 0.6 mg  $\text{O}_3$ /mg  $\text{DOC}_0$ . With respect to the coagulant dosage, the best results were observed at the highest applied concentrations. A combination of 0.5 mg  $\text{O}_3$ /mg  $\text{DOC}_0$  and 8 mg  $\text{Fe}^{3+}$ /L leads to a total reduction down to < 5 % of the initial colloid content (Schulz optimum). The combination of pre-ozonation with subsequent coagulation shows the potential to decrease the necessary usage of coagulants, which leads to a reduction of sludge disposal and solid load when this combination is applied as a pre-treatment for membrane systems. The impact on particle stability of other parameters, like pH, ionic strength, concentration of alkaline ions, during these treatments should be investigated in future tests for a further optimization of colloid removal.

In the second part of the study, pre-treatments impacts were evaluated not only on the particle removal but also on the UF-filtration performance. Specific ozone dosages of 0.5-0.8 mg  $\text{O}_3$ /mg  $\text{DOC}_0$  in combination with coagulation were observed to reduce the total fouling resistance of about 65-75 %, compared to the untreated secondary effluent. In filtration tests of different pretreated samples, a linear correlation was observed between the content of colloids < 200 nm measured by NTA and the total fouling resistance during ultrafiltration at lab-scale. Compared to other water quality parameters, which are generally associated with low pressure membrane fouling, the best prediction on fouling potential was given by colloid fraction < 200 nm.

However, an ozone-induced increase of irreversible fouling was detected during the lab-scale experiments with the applied PES membrane. A linear relationship between the applied ozone consumption and the resulting irreversible fouling resistance was determined, which is suggested to be a result of specific adsorption of the formed small, hydrophilic molecule fragments and the hydrophilic membrane material. For an improved understanding of this behaviour, further tests are required to assess the effect of ozonation in long term trials with other membrane materials and several pore-sizes. These modifications are believed to be

responsible for irreversible fouling due to pore constriction and adsorption onto and into the membrane matrix. An assessment of the irreversible fouling by NTA was not possible, especially when ozone was applied. The detection limit of the instrument is at 50 nm for that type of water with the nominal pore size of 26 nm for the applied UF-membrane. The outcomes of lab-scale tests were confirmed by an online colloid monitoring at an UF-pilot plant. A direct prediction of irreversible fouling could not be made.

Furthermore, in pilot-scale operations a range of factors like applied flux, operational conditions and cleaning efficiency influence the fouling of the membrane system. Therefore, not all reversible fouling effects could be explained by submicron particle measurement. However, regarding the water quality and the complexity of the fouling phenomena, the submicron particle measurement seems to be an adequate and promising method for a rapid and reliable assessment of the total fouling potential of the water.

Optimizing the online measurement would offer the opportunity to couple the chemical dosing and the colloid concentration. One possible option may be an operation with constant ozone consumption of 0.5 mg O<sub>3</sub>/mg DOC<sub>0</sub> and a colloid-volume proportional coagulant dosing, thus lowering the operational costs as well as the solid load on the membrane surface when the water shows less fouling potential.

## Chapter 4 Monitoring of micro sieve performances

### 4.1 Selection of the suitable device

There are many analytical bulk parameters to express the solids content of water. Among the most frequently used are: Total solids (TS), Total Suspended Solids (TSS), Particulate Organic Carbon (POC=TOC-DOC), Volatile Suspended Solids (VSS), Turbidity, particle number, Zeta potential... During first test trials, devices measuring these parameters were tested at TUB by KWB workers to check their reproducibility and reliability. They were analyzing the real effluent of the WWTP Ruhleben and characterizing particle properties, e.g. size, and surface characteristics, to control the coagulation and flocculation efficiency. The most suitable device to monitor this pretreatment step was selected for long term experiments, namely a particle counter working with the light extinction principle. The goal of this instrument is to optimize the coagulation and flocculation steps of the micro sieve pilot plants as well as the microsieve operation. Its efficiency is compared with turbidity sensors installed online in the pilot plant.

### 4.2 Materials and methods

#### 4.2.1 Particle counter: characteristics, principle of light extinction

##### 4.2.1.1 Characteristics of the WaterViewer

All experiments were carried out with the Pamas WaterViewer particle counter. The WaterViewer works according to the principle of light extinction. It consists of a sensor type HCB-LD-25/25 (see characteristics in the Table 6) design to analyse high polluted sample, and of a Sensor Flushing Unit for automatic cleaning with a 1% HCl solution. The sensor had to be washed with 40 – 70% ethanol before storage for a long period.

Table 6: Characteristic of the WaterViewer

<b>Sensor type</b>	<b>Cell size</b>	<b>Nominal flow rate</b>	<b>Max concentration including a coincidence rate of less than 8 %</b>	<b>Potential interval of detection</b>	Potential interval of detection
	<b>µm</b>	<b>mL/min</b>	<b>P/mL</b>	<b>µm</b>	<b>µm@</b>
<b>HCB-LD-25/25-620</b>	250x250	25	120 000 P/mL	1-200	4-170

The device was provided with software to program the measurement series as well as the cleaning frequency. The different options available with this program are presented in Annex 1).

##### 4.2.1.2 Principle of the light extinction

The liquid flows through the measuring cell of the sensor. A light beam enters the measuring cell on one side, on the other side there is a photo-detector (see Figure 17). The illumination source

is a laser diode. If the liquid is clean and pure, then the light will pass through the measuring cell without putting any trace or shadow on the photo-detector. However, if there are particles in the liquid, then the light beam hits the particles and as a result, the shadow of the particle is shown on the photo-detector. The surface of the shadow causes a voltage change on the photo-detector and indicates the size of the particle flowing through the sensor cell. The particle counter transfers the number of shadows on the photo-detector into the quantity of particles in the liquid. Projecting the shadow on the photo diode means eliminating the third dimension of the particle. The photo diode with its integrated light-sensitive surface reduces the now two-dimensional shadow picture again to a one-dimensional signal which is proportional to the cross section. The correspondence of the sensor signal and the particle sizes is done at the calibration. The electrical signal is translated into the particle diameter. Furthermore, the particle sizes are distributed in different size classes. The sensor specification tells us the flow rate of the sensor and the corresponding liquid volume. With the help of this specific flow rate, a calibrated particle counter is able to indicate the particle concentration of the liquid – even individually for different particle sizes. If the software provides cumulative results then the particle concentration for each size range will be the particle concentration for all particles above a given size, for example: > 1  $\mu\text{m}$ , > 3  $\mu\text{m}$ , > 5  $\mu\text{m}$ , > 10  $\mu\text{m}$ , > 20  $\mu\text{m}$ , > 40  $\mu\text{m}$ , > 80  $\mu\text{m}$  and > 160  $\mu\text{m}$ . If the software provides differential results, then the particle concentration is given for a range, for example: 1 < < 3  $\mu\text{m}$ , 3 < < 5  $\mu\text{m}$ , 5 < < 10  $\mu\text{m}$ , 10 < < 20  $\mu\text{m}$ , 20 < < 40  $\mu\text{m}$ , 40 < < 80  $\mu\text{m}$ , 80 < < 160  $\mu\text{m}$  and 160  $\mu\text{m}$  <.

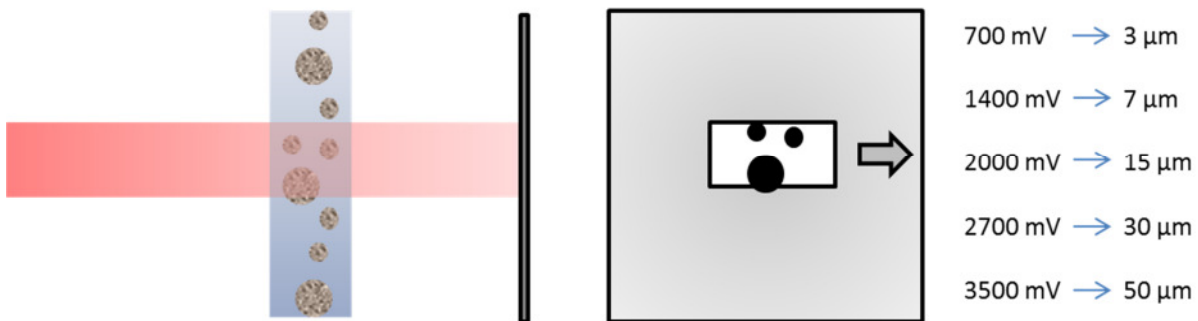


Figure 17: Principle of light extinction

#### 4.2.1.3 Statistics of the measurement results

The reproducibility of measurements depends on the particle count; the measuring time therefore should not be too short – especially when analysing clean fluids. Apart from quantity and measuring time, the shape of the particles also has an influence on the detected size and the reproducibility of the measurements. If the particles are non-spherical, the size is detected differently depending on the orientation. Non-spherical particles, such as flat or filamentary shapes might lead to unsteady measuring results.. This case however is rare, because very small particles by nature are mostly spherical.

Definition of coincidence: The statistical relevance of the measuring results is limited only by the maximum particle concentration which itself depends on coincidence. In case of coincidence, more than one particle is in the laser beam at the same time. To allow a definite correlation between particle size and threshold value, only one particle should be in the laser beam. If more

particles are at the same time in the laser beam, the total extinction of the light is assigned to one particle size. Fewer, but larger particle are detected.

#### 4.2.1.4 Advantages and disadvantages of this technique

##### **Advantages**

- Online measurements for a longer period of time
- Measuring results reliable and repeatable
- Measurement is quick and simple, allowing automation
- Calibration with standard latex particles

##### **Drawbacks**

- With highly concentrated samples, the detection of each particle is underestimated because of coincidence: two small particles are detected as one large particle
- Bubbles may be interpreted as particles and counted as well.
- Only a quantitative measurement of particles and their sizes is possible; a qualitative measurement showing the chemical composition of the particles is not possible

#### 4.2.2 Lab equipment

##### **Water**

The influent water of the pilot plant or of the Jar-Test was the effluent of the WWTP Ruhleben, also called secondary effluent.

##### **Coagulant**

Two metal salts were used: iron (III) chloride ( $\text{FeCl}_3$ ) and polyaluminium chloride (PACl).  $\text{FeCl}_3$  was dosed between 4 and 5 mg Fe/L and PACl between 1.9 and 2.9 mg Al /L.

##### **Polymer/Flocculant**

Cationic polymer with high molecular weight was used for the flocculation with dose between 0.5 and 2 mg/L.



##### **Filtration**

The coagulated and flocculated water was filtered with a Hydrotech test tube through a filter cloth (mesh size 10  $\mu\text{m}$ ).

##### **Jar-Test**

Different operating conditions were tested with the aid of jar tests. All jar tests were conducted according to the DVGW worksheet W 218. For the jar test 1.8 L of pilot plant influent are filled into a 2 litre beaker equipped with a stator and a stirrer. The coagulant is added at 400 rpm. The rapid mixing lasts 10 sec. Afterwards the mixing velocity is reduced to 50 rpm. After 4 minutes of slow mixing the polymer is added at 200 rpm. Again the rapid mixing lasts 10 sec and is followed by 4 min of slow mixing at 50 rpm. Then 0.8 litres of the treated water is poured into the test tube and passes the mini microsieve (Figure 18). The filtration is finished after 1 min.

**Figure 18: Jar-Test apparatus**

**Analytics** See 3.2.2 Analytics

#### 4.2.3 Pilot plant: online implementation

The micro sieve pilot plant built by HYDROTECH is installed at the Ruhleben STP and fed out of the secondary clarifier effluent. The same coagulants and flocculants were tested in the laboratory and in the pilot plant (see 4.2.2). The pilot plant is dimensioned for 10 to 30 m<sup>3</sup>/h and a maximum suspended solids concentration in the influent water of 20 mg/L. The particle counter was implemented directly at the effluent pipe of the pilot plant (see

Figure 19). The particle counter pumps 25 mL of effluent per min analyzing the sample in real time. A bottle of 1% acid solution is connected to the instrument to automatically clean the pipes and the measuring cell of the device every 30 minutes.

Figure 19: Picture of the particle counter in the pilot plant

### 4.3 Lab results

#### 4.3.1 Reproducibility and reliability of the device

Four solutions of standard particles (SP) (50 µm) at 4 different concentrations were prepared to be analyzed with the particle counter. In the first, 5 drops of SP were mixed in 500 mL of distilled water, in the second 10 drops, in the third 20 drops, and then 30 drops in the last one. Results are presented in

Figure 20).

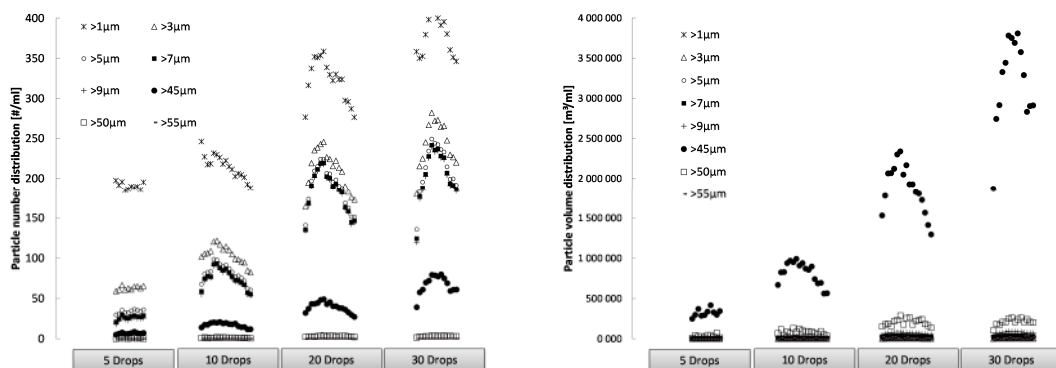


Figure 20: Standard particles (50 µm) at different concentrations: a) number, b) volume distribution

Because the number of small particles is far higher than the numbers of the largest one, the particle size distribution cannot be used to measure an absolute value of the particle size in a solution (

Figure 20a). However using the particle counter device results to show the volume distribution of particles in solution allow the user to detect the main particle size in a sample (

Figure 20b).

The volume distribution of 50 µm particles in solution shows that particles with a size above 45 µm are the most common in the sample which validates the reliability of the device at least to analyze solutions with standard particles. The relative concentration between all samples can also be calculated: the concentration increases with a factor 2.5, 2.3 and 1.7 between the samples 2 and 1, 3 and 2 and finally 4 and 2 (respectively). The theoretical concentration factors are: 2, 2 and 1.66 which shows the qualitative reliability of the measurement device.

Results from the particle counter were very reproducible if the device sensor and the pipes were cleaned without adsorption or attachment of the sampling material. A sample measured during one day shows no reproducible results due to the accumulation of the particles attached to the wall of the PVDF pipes. In this case, the particle count measured for each particle size ranges were decreasing over the time with some release of particles detected from time to time. The automatic cleaning device was not always sufficient to diminish this effect. The particle counter had to be regularly cleaned to improve the results quality. This was the most difficult part to operate online the particle counter: how to get a representative sample to the device measuring cell?

To avoid accumulation of particles in the piping system, a cleaning protocol was followed. Automatic online cleaning with distilled water for 1 minute every 10 minutes and a daily manual cleaning with distilled water, an acid solution (1% HCl) and air pressure.

#### **4.3.2 Comparing influent and effluent water quality**

Two beakers of 1 L were prepared and analyzed by the particle counter. The first contained the influent water of the microsieve pilot plant. The second contained the effluent water of a Jar Test (JT). For the JT, the coagulant dose was 5 mg Fe/L of iron chloride, the polymer dose was 2 mg/L of active material from the cationic polymer CP261FS and the filtration was carried out with a 10 µm filter. Results are presented in the Table 7.

**Table 7: Particle count and particle removal before and after Jar-Testing**

<i>Particle count (particles/mL)</i>	<i>&gt; 1 µm</i>	<i>&gt; 2 µm</i>	<i>&gt; 4 µm</i>	<i>&gt; 8 µm</i>	<i>&gt; 10 µm</i>	<i>&gt; 15 µm</i>	<i>&gt; 20 µm</i>	<i>&gt; 50 µm</i>
Influent	30059	18982	12215	4531	746	181	55	6
Effluent	3562	1564	751	169	22	2.5	0.2	0
Removal [%]	88	92	94	96	97	99	99.7	100

After pre-treatment and filtration at 10 µm, more than 97% of the particles above 10 µm are removed from the water. The larger the particles, the higher is the percentage of removal. Particles below 10 µm are also removed to a large extent due to the coagulation and flocculation effects: 82% of particles between 1 and 2 µm are removed from the secondary effluent. This table shows the efficiency of this process: coagulation, flocculation and microsieve 10 µm filtration as tertiary treatment.

#### **4.3.3 Comparison of coagulant type: iron and aluminium, effect of pH**

Six samples were prepared with 2 coagulant types: iron chloride ( $\text{FeCl}_3$ ) and polyaluminium chloride (PACl). The coagulants were mixed in distilled water at the same concentration: 0.071 mmol Me /L. For each coagulant, 3 different pHs were tested: pH = 7, 6 and 4. The particle

counter was used to analyze the particle size distribution of these 6 samples and to check which kind of coagulant produces the highest amount of suspended solids.

**Table 8: Comparison of particle count for different coagulant types at different pH**

Coagulant type	$FeCl_3$	$FeCl_3$	$FeCl_3$	$PACl$	$PACl$	$PACl$
Coagulant dose [mg Me/l]	4	4	4	1.9	1.9	1.9
pH	6.9	6	4	7.1	6	4
Particle count mean [/mL]	10100	1500	680	1850	1850	865

The optimum particle removal by sweep flocculation occurs in the pH range 7 – 8.5 with the Al dose applied and in the pH range 6 – 8 with the Fe dose applied (Amirtharajah and Mills, 1982). Sweep coagulation takes place when raw water colloids become enmeshed in a voluminous precipitate gained from aluminium or iron coagulants. The bulk precipitate is a heterogeneous mix of trihydroxides ( $Me(OH)_3$ ) and small polycations. The trihydroxide precipitates are detected by the particle count as shown in the Table 8. At an optimal pH for the  $FeCl_3$  (6.9), the particle number is higher by a factor 7 than the particle number measured in the solution at a pH 6, (the limit of the sweep coagulation pH range). The lower the pH, the lower is the particle number detected by the device because the hydrolytic reactions form a variety of soluble mononuclear and polynuclear Al and Fe-species. Moreover the structure of the precipitated iron is more compact and inert than the amorphous nature of precipitated alum. Therefore the iron particles are better detected by the particle counter than the aluminium particles.

#### 4.3.4 Postflocculation analysis

The pilot plant was operated with 4 mg Fe/L for the coagulation, 2 mg/L CP 261 FS for the flocculation, a mesh size of 10  $\mu m$  and an influent flow of 20  $m^3/h$ . After a few days of operation, postflocculation occurred in the permeate tank as well as in the permeate pipes. This postflocculation was due to residual coagulant and polymer in the effluent after the filtration. To measure this postflocculation effect, 1L of the microsieve pilot plant effluent was filled in a beaker and measured with the particle counter overnight (see Figure 21). The experiment was repeated 3 times. Differential results are displayed on Figure 21.

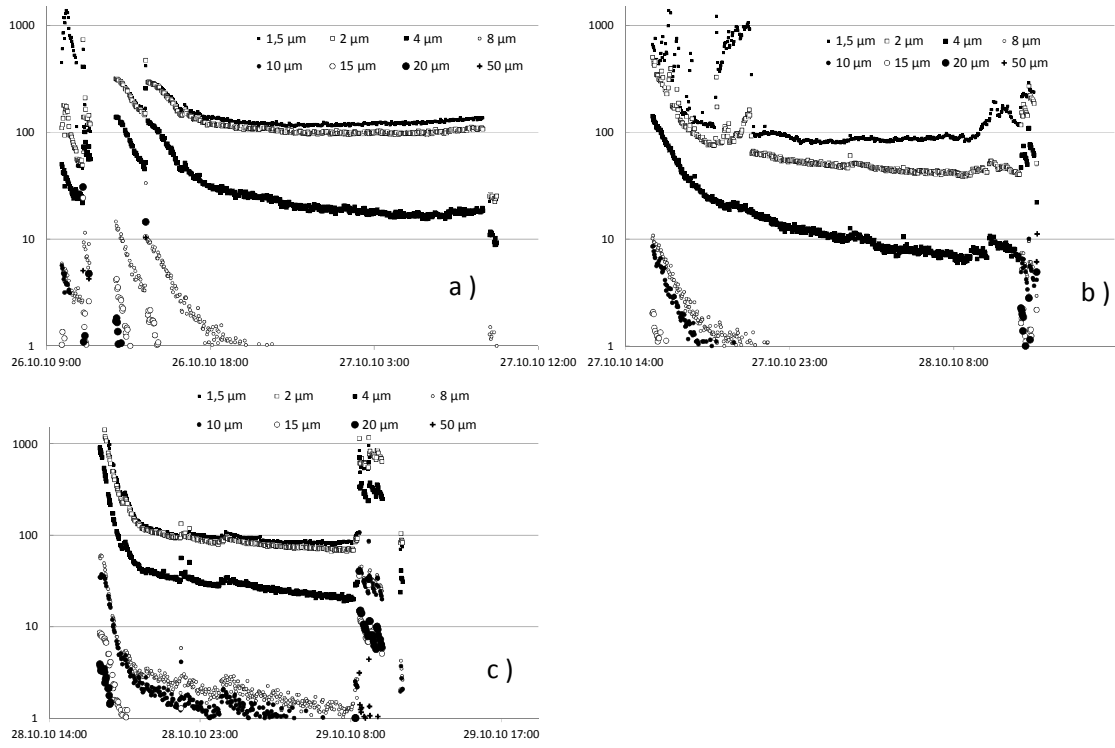


**Figure 21: Postflocculation experiments without automatic cleaning a) 26.10.10, b) 27.10.10, c) 28.10.10**

The particle number measured by the device decreases continuously during the first 6 hours of the experiment. Then no particles larger than 8  $\mu\text{m}$  were detected anymore. The number of the smallest particles stayed constant over 14 hours (see Figure 21a). As no automatic cleaning device was installed and the sample was not mixed, larger particles attached to the wall of the pipes and the beaker and did not reach the device sensor. Therefore after a while only the particles below 8  $\mu\text{m}$  were detected by the particle counter.

The following day, Figure 21b, the experiment was repeated. The same results were obtained except in the morning. When the operator arrived, the beaker was mixed to put the particles back in suspension. The amount of larger particles analyzed then increased suddenly. Particles larger than 20  $\mu\text{m}$ , not detected at the trial beginning, were measured by the instrument in the morning. In general the solution contained larger particles at the trial end and fewer particles smaller than 4  $\mu\text{m}$ . It confirms that postflocculation occurred during the night. Similar results were observed during the third trial, Figure 21c.

To study this phenomenon in more detail, an automatic cleaning was installed and the sample was continuously mixed with a magnet stirrer. Differential results are presented Figure 22.

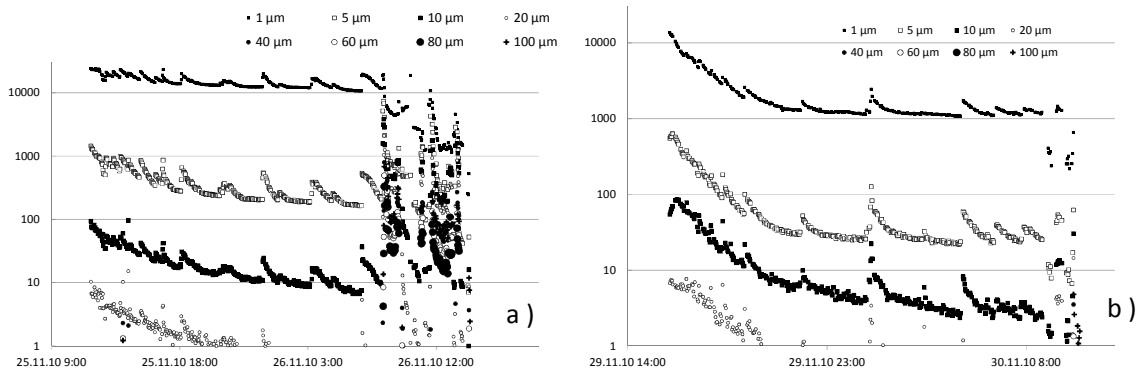


**Figure 22: Postflocculation experiments with automatic cleaning**

The sample was analyzed 5 times during 2 minutes and cleaned for 5 minutes with distilled water of an acid solution (1% HCl) and then analyzed again, and so on. Each cycle took around 15 minutes. The particles numbers decreases over the time but more slowly than in the previous experiments. Due to the automatic cleaning we can also observe some release of particles from time to time. But after 10 hours (Figure 22a) or 5 hours (Figure 22b) no particles above 40  $\mu\text{m}$  were detectable. Manual mixing at the trial end brought large particles (40 – 400  $\mu\text{m}$ ) back in suspension as shown on Figure 22.

These 5 experiments show clearly that postflocculation of the effluent water occurs after several hours (time depending on the sample). However the phenomenon cannot be observed accurately with an online particle counter due to the system of pipes and the beaker needed to bring the sample to the sensor measuring cell.

#### 4.3.5 Fractionation tests

To characterize the effluent water of the pilot plant and find the best operating conditions for the pilot plant, fractionation tests were carried out. Coagulated and flocculated water was taken from the flocculation tank (FT) and filtered in the lab (Hydrotech test tube) through different mesh sizes: 10, 15, 18 and 25  $\mu\text{m}$ . Samples were analyzed with the particle counter. The total phosphorus (TP) concentration, the residual aluminium (Al) concentration and the filtration velocity were measured in parallel. Results are presented Figure 23 and Figure 24.

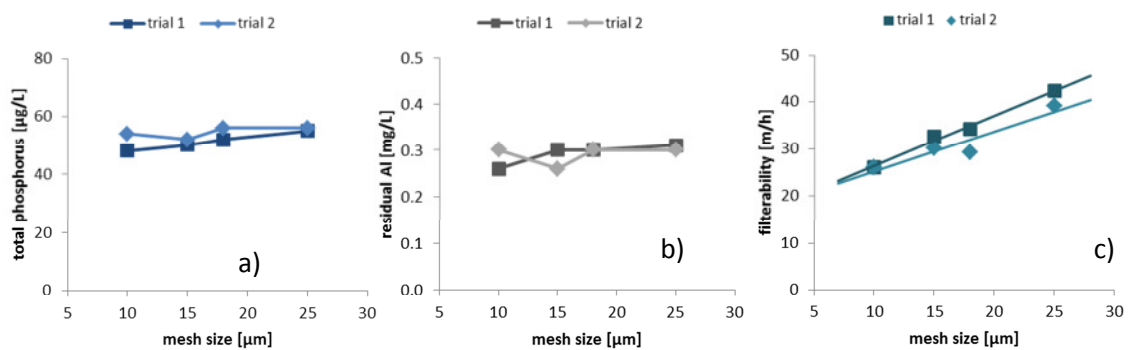


**Figure 23: Lab analysis results of the fractionation tests a) TP, b) residual Al, c) filterability**

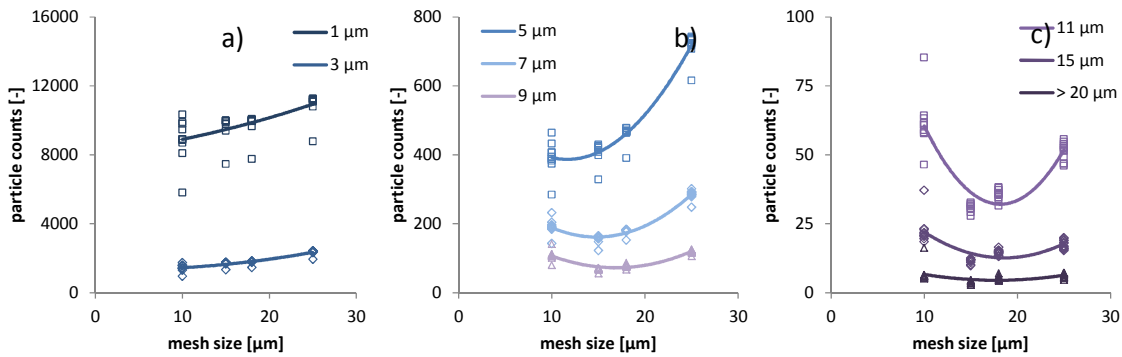


**Figure 24: Differential particle count results of the fractionation test for particle sizes between a) 1 μm > >5 μm, b) 5 μm > >11 μm, c) 11 μm > >200 μm**

The total phosphorus concentration and the residual aluminium concentration in samples after filtration were very similar: between 45 and 60 µg/L for the TP and 0.25 and 0.3 mg/L for the residual Al whatever the filter mesh size used (Figure 23a & b). The larger the mesh size, the higher was the filtration velocity from 25 m/h at 10 µm to 40 m/h at 25 µm (Figure 23c). The right mesh size choice for the microsieve pilot plant is a compromise between the effluent quality goals and the total cost of the process. The higher is the filtration velocity, the less will be investment and operational costs.

Particle count results are more accurate than the TP and Al concentration and could help to decide which mesh sizes would be the most suitable. The filtration with 25 µm mesh size resulted in the highest particle counts for particles > 11 µm. The proportion of particles with a size between 5 and 11 µm was higher by a factor 2 compared to samples filtered at lower mesh sizes (Figure 24b). In the lab it did not have any influence on the phosphorus or aluminium concentration but in the pilot plant, where the shear forces are higher; these particles would pass through the filter media with phosphorus and aluminium attached and decrease the effluent water quality.

The filtrate of the 10 µm filter media contained more particles in the range of 7-15 µm compared to the filtrate of the 15 or 18 µm filter media. The 10 µm filter media has fewer filter openings and thus higher fluxes through the pores. Most probably the higher shear forces result in more floc breakage.

With a total phosphorus effluent concentration below 80 µg /L as goal, it was recommended to test the 18 µm filter media in the pilot plant to decrease the cost of this process and keep a similar effluent quality as with 10 µm. The 25 µm filter media would most probably lead to a phosphorus concentration higher than 80 µg /L as well as a higher residual aluminium concentration.

#### 4.4 Pilot plant results

##### 4.4.1 Results repeatability

**Table 9: Particle counter repeatability**

	1 - 3 μm	3 - 5 μm	5 - 7 μm
--	----------	----------	----------

8.3.12 10:49	5244.24	814.88	127.36
8.3.12 10:50	5170.72	809.68	122
8.3.12 10:50	5202.96	800.8	131.44
8.3.12 10:51	5209.28	796.56	130
8.3.12 10:51	5164.88	780.48	128.72
8.3.12 10:52	5211.44	792.72	127.52
8.3.12 10:52	5166.48	806.16	131.76
8.3.12 10:53	5228.88	801.44	130.08
8.3.12 10:53	5218.8	792.96	127.68
8.3.12 10:54	5155.76	801.76	125.2
8.3.12 10:56	5198.24	791.6	125.52
Std	29.11	9.56	2.92
Mean	5197.43	799.00	127.93
% error	<b>0.56%</b>	<b>1.20%</b>	<b>2.29%</b>

The Table 9 presents the particle counter results measuring the same sample during 7 minutes. According to ISO 11171 (calibration for optical particle counter) the error limit for all measurements with a quantity of more than 10 000 particles is 5.5 %. Measurements of the particle concentration in a secondary effluent with the Waterviewer show error measurements below 2.3%. This device produces repeatable results.

#### 4.4.2 Influence of the influent flow

The micro sieve pilot plant was operated with a daily flow pattern between 10 and 23 m<sup>3</sup>/h. The coagulant dose was 2.4 mg Al/mL and the polymer dose was 2 ppm. Figure 25 shows the impact of the influent flow on the effluent water quality measured online by a particle counter.

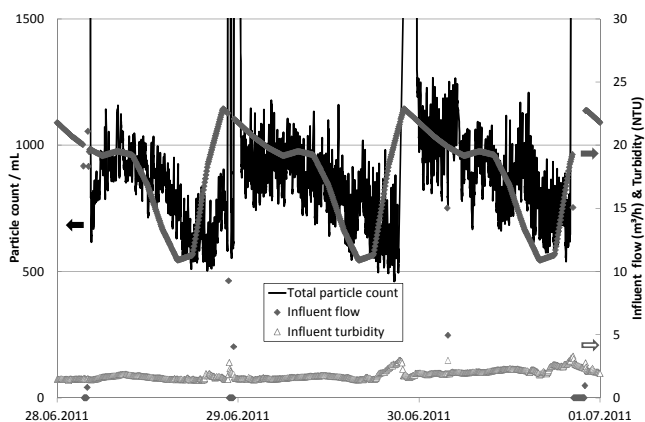
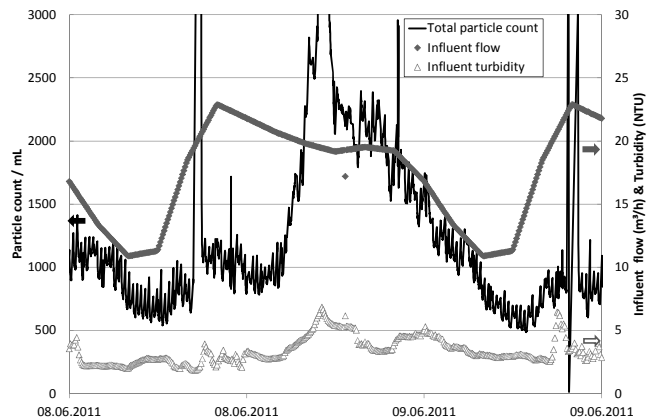


Figure 25: Impact of the influent flow on the effluent water quality

At low influent turbidity between 2 and 4 NTU, the influent flow has a detrimental effect on the effluent water quality. The higher the influent flow, the higher is the number of particles in the effluent. A lower hydraulic retention time (HRT) for the coagulation and the flocculation at higher flow could cause this effluent particle concentration increase. The flocs are probably smaller and less stable in comparison to those formed during a longer HRT. Moreover a higher influent flow leads to a higher shear force during the filtration step which might be strong enough to break more flocs, which then pass through the 10 µm filter.

A similar trial was carried out at higher influent turbidity. The operating conditions were otherwise exactly the same: daily flow pattern, same coagulant and polymer dose and type. Results are presented in the Figure 26.



**Figure 26: Impact of the influent flow on the effluent water quality**

The variation in the influent turbidity has a stronger impact on the particle count in the effluent than the influent flow. An increase of 2-3 NTU in the influent turbidity (from 3 to 6 NTU) leads to an increase of the particle number by a factor 3 (from 1000 to 3000 particles/mL).

To conclude, to operate the micro sieve pilot plant, the influent turbidity is a significant parameter to take into account. It is important to monitor this parameter to improve the coagulation and flocculation steps. The chemical dose should be adapted to the influent water quality.

A higher influent flow leads to a slightly decrease in the effluent quality but the influent flow between 10 and 23 m<sup>3</sup>/h plays a minor role for the optimization of the micro sieve process.

#### 4.4.3 Effluent water quality with and without pre-treatments

The particle counter measured the particle size distribution in the pilot plant effluent with and without pre-treatments. The goal was to show the efficiency of the pre-treatments regarding the effluent water quality. The flow was 20 m<sup>3</sup> /h. With pre-treatments, the water was coagulated with polyaluminium chloride (2.4 mg Al/L) and flocculated with cationic polymer (2 mg /L). The Figure 27 shows the particle count in the effluent of the micro sieve with and without pre-treatments.

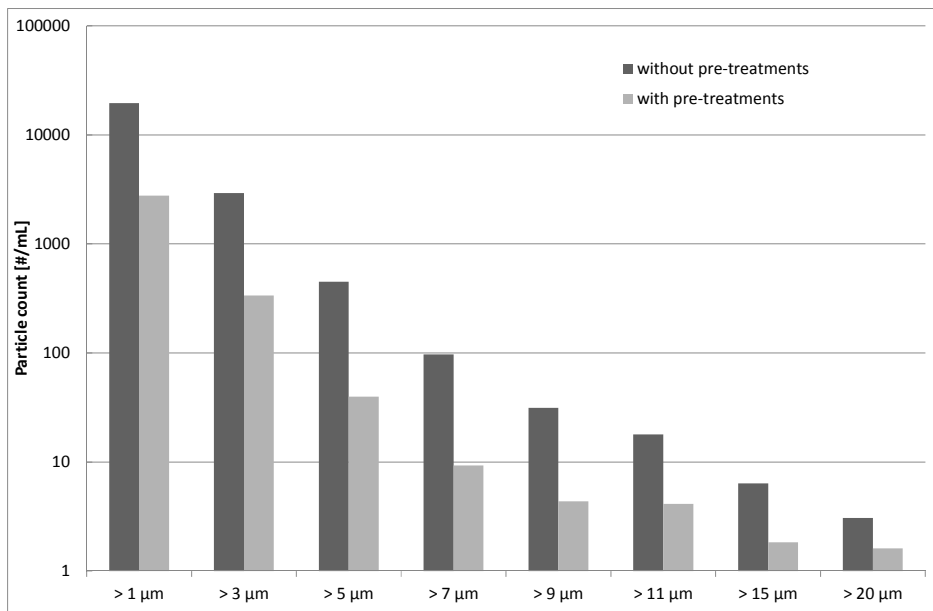


**Figure 27: Impact of the pre-treatments on the effluent water quality.**

The particle count in the effluent was reduced for all particle size ranges by a factor between 2 and 12 when the pilot plant was operated with pre-treatments. This figure shows the importance of coagulation and the flocculation to achieve a good water quality.

#### 4.4.4 Optimization of the coagulation: type, dose, mixing and hydraulic retention time

##### 4.4.4.1 Coagulant types and doses

Experiments were carried out for 2 weeks with the pilot plant at a flow of 20 m<sup>3</sup> /h. During the first week, an increased iron chloride concentration was dosed between 2 and 10 mg Fe /L before flocculation with 1.5 mg/l of cationic polymer CP261FS. During the second week, an increased polyaluminium chloride concentration was dosed between 1 and 5 mg Al /L before flocculation with 1.5 mg/l of cationic polymer CP261FS. The goal was to find the optimal operating conditions for the pilot plant. Results are represented on Figure 28.

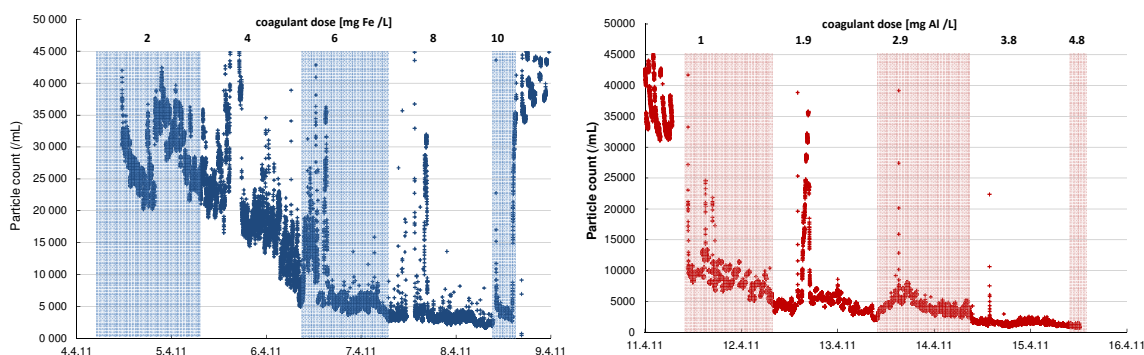


**Figure 28: Particle count for an increasing a) iron chloride dose and b) polyaluminium chloride dose**

The two figures present the total particle count of particles between 1 and 200 μm per millilitre versus the time. The coagulant dose applied for each day is indicated at the top of the graphs.

A general comment is that the higher the coagulant dose, the lower is the particle number measured in the effluent. But the interpretation is moot, because with a higher coagulant dose, a higher post flocculation effect is observed. More suspended solids pass through the filter and agglomerate themselves in the effluent tank or in the pipes before the measuring cell of the particle counter. The particle number is smaller but because flocs are larger, the amount of solids is higher but cannot be detected by the measuring device. The question is whether the particle concentration is lower because of the formation of optimal flocs due to an optimal dose applied or because of post flocculation which catches the particles before the device sensor. The formation of a cake layer at the panel surface could also explain the lower particle concentration at high chemical dose. However it was observed that more suspended solids passed through the filter panels at high chemicals doses (above 6 mgFe/L and 3 mgAl/L).

The effluent particle concentration without chemicals applied is between 35000 and 100000 particles per millilitre and with 2 mg Fe/L between 20000 and 40000 /mL. It means that 2 mg/L is not enough to form good flocs retained by the filter media. With 4 mg Fe/L, the particle number decreases from 30000/mL to 10000/mL and with 6 mg Fe/L, this number decreases further to 5000/mL. A higher iron chloride dose does not have a significant effect on the effluent particle concentration. Moreover, the backwash time was above 66% which showed that the solid load on the pilot plant was too high. It indicates an optimal iron chloride dose between 4 and 6 mg Fe/L.

The effluent particle number after coagulation with polyaluminium chloride is a lot lower, around 10000/mL, even with a low aluminium dose. This is due to the floc characteristics which are less detectable by the instrument (see C3.3) but also probably by the stronger flocs formed by the PACl in our case which lead to less suspended solids in the effluent. During this trial a dose of 3.8 mg Al/L provokes an increase of the post flocculation effect and of the backwash time up to 100 %. It indicates an optimal polyaluminium chloride dose between 1.9 and 2.9 mg Al/mL.

The use of a particle counter is not recommended to optimize the coagulant dose due to the accumulation of suspended solids in the pipes which gives unrealistic particle concentration values. A standard turbidity sensor was better able to detect the same trends than the Waterviewer during this trial.

#### 4.4.4.2 Coagulant mixing velocity

The operating conditions for this trial was a 20 m<sup>3</sup>/h flow, coagulation with 2.4 mg Al/L, flocculation with 2 mg/L of a cationic polymer and a 10 µm filtration. The mixing velocity in the coagulation tank was increased from 18 to 46 rpm. The particle counter analyzed online the total particle number in the effluent. Results are presented Figure 29.

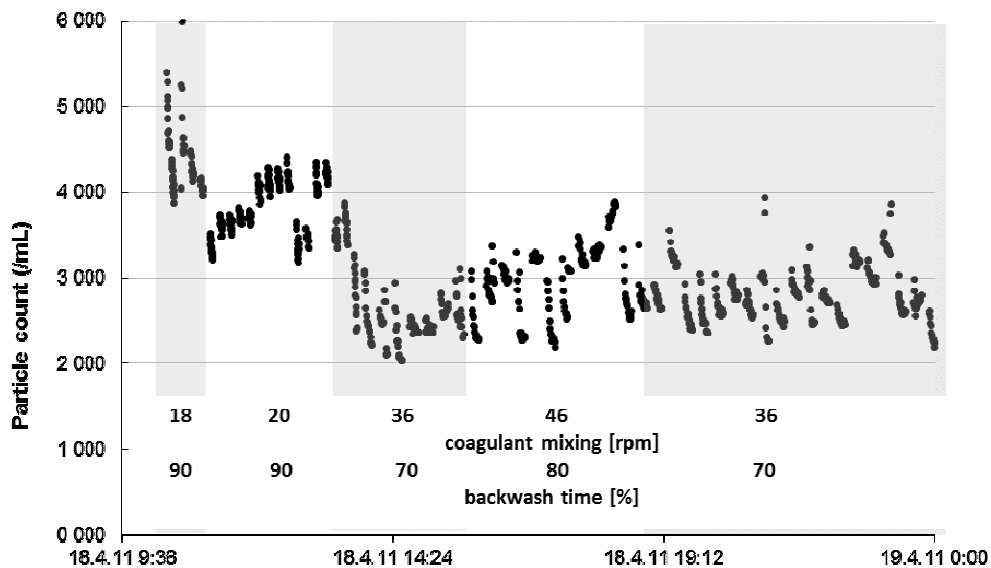


**Figure 29: Increase of the mixing velocity in the coagulation tank**

This trial showed an optimum at 36 rpm, the total particle concentration was the lowest (around 2000 – 3000) as well as the backwash time (70%). An increase of energy input would not increase the effluent water quality. The other parameters such as the turbidity and the total phosphorus concentration in the effluent were not able to detect this optimum. This case shows the value and the reliability of the online particle counter device to optimize a process such as a microsieve filtration.

#### 4.4.4.3 Coagulation hydraulic retention time

In the pilot plant, it was possible to modify the coagulant tank volume between 1.44 and 2.16 m<sup>3</sup>. At 20 m<sup>3</sup>/h, the hydraulic retention time (HRT) was 4 - 6.5 minutes. Particles count was measured online but data showed no clear trends to optimize this HRT. The backwash time was a better indicator.

### 4.4.5 Optimization of the flocculation: type, dose, mixing and hydraulic retention time

#### 4.4.5.1 Flocculant types and doses

Figure 30 presents the particle concentration in the microsieve effluent with increasing coagulant and polymer dose. The flow was around 15 m<sup>3</sup>/h and the chemical dosing was proportional to the influent ortho-phosphate and turbidity concentration. The polyaluminium chloride concentration rises from 1.9 to 2.2 mg Al/L and the cationic polymer from 0.56 to 0.77 mg/L. During this trial period, the influent turbidity varied between 1.84 and 3.11 NTU and tended downwards.

The effluent turbidity values followed the influent turbidity trends, whereas the effluent particles concentration followed the influent turbidity at constant chemical dosing but tended to increase with increasing chemical dosing. For example when the coagulant dose went from 1.93 to 2.06 mg Al/L along with the polymer dose from 0.56 to 0.61, the particle concentration

increased from 5765 particles /mL to 11128 particles /mL. After 10 minutes at constant chemicals doses, the particle count decreased again to 6945 particles /mL probably caused by the formation of a cake layer either on the filter panel or on the piping system leading to the particle counter cell. This phenomenon (increase of chemicals dose and stabilization) occurred 3 times during this trial period with the same impact on the particle counter results. To conclude, the particle counter was in this case more sensitive than the turbidity sensor in the effluent. It was possible to detect an increase of suspended solids in the effluent due to more chemical products dosed whereas the turbidity sensor was not able to do it.

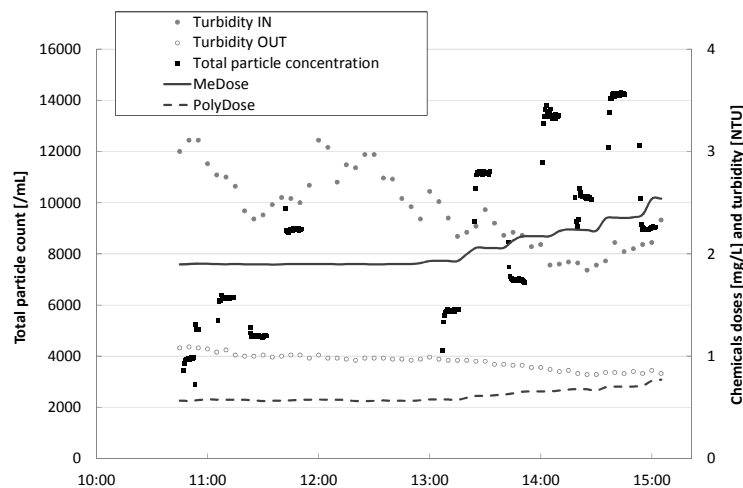


**Figure 30: Impact of chemicals doses increase on the effluent water quality**

Two similar cationic polymers with high molecular weight were tested in the pilot plant: the Fennopol and the CP261FS. Their effect on effluent particle counts was evaluated under two operating conditions (see Figure 31). For the first trial series, 4 mg Fe/L of iron chloride was dosed with 1.5 mg/L of polymer (see Figure 31 a + b). For the second trial series, 2.4 mg Al/L of polyaluminium chloride was dosed with 2 mg/L of polymer (see Figure 31 c + d). Other parameters were similar for all trials: flow at 20 m<sup>3</sup>/h, influent turbidity and water quality varying in the same range.

In both cases, the total particles concentration was in the same range for both flocculant types: between 12000 and 30000 with iron as coagulant and between 1000 and 3300 with aluminium based coagulant. Both flocculants presented the same performances but results with Fennopol as polymer seem to be more stable. It could be that flocs built with the Fennopol are slightly stronger and more stable.

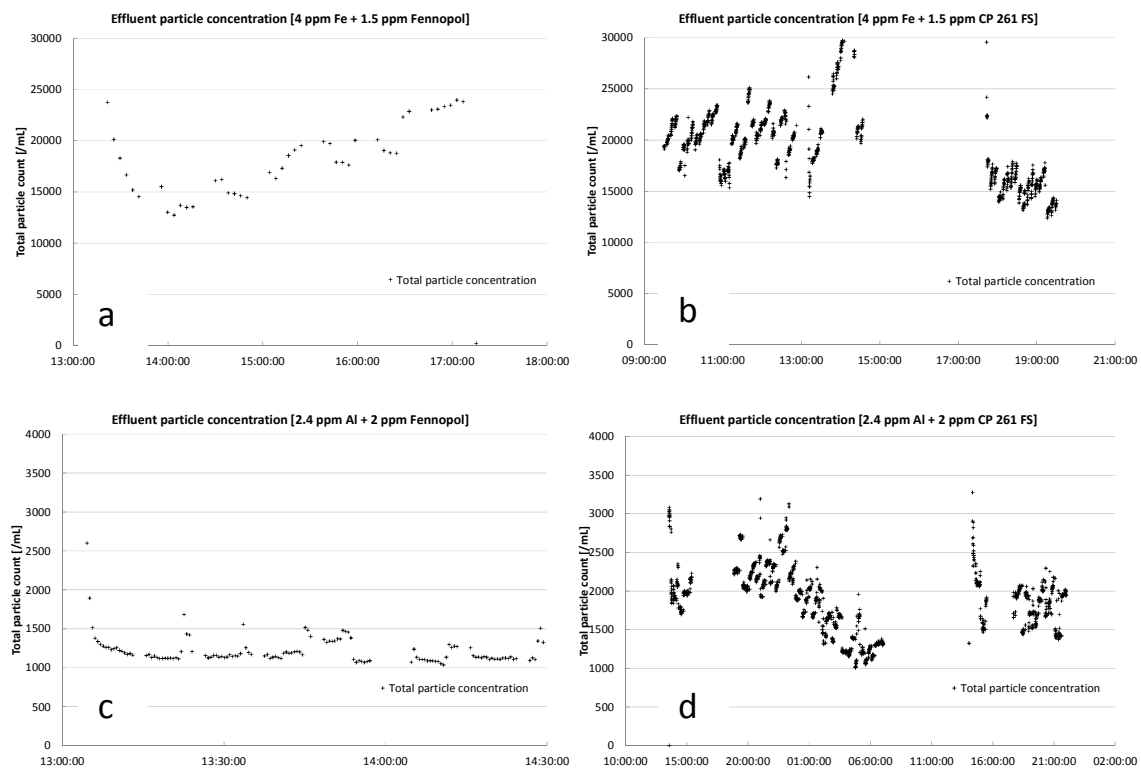


**Figure 31: Impact of the flocculant type on the total particle count in the microsieve effluent**

At the end of these trials, it was recommended to keep working with the Fennopol as polymer and not with the CP261FS. The decision was taken according to the backwash values of the pilot plant and not according to the particle counts. In this case, the backwash parameter was more decisive than the particle count. It highlights the importance of having a group of key parameters which complement each other to optimize a process.

#### 4.4.5.2 Flocculant mixing velocity

The operating conditions for this trial was a flow of 20 m<sup>3</sup>/h, coagulation with 2.4 mg Al/L, flocculation with 2 mg/L of a cationic polymer and a filtration at 10 µm. The mixing velocity in the flocculation tank was increased from 18 to 45 rotations per minutes (rpm). The particle counter analyzed online the total particle number in the effluent.

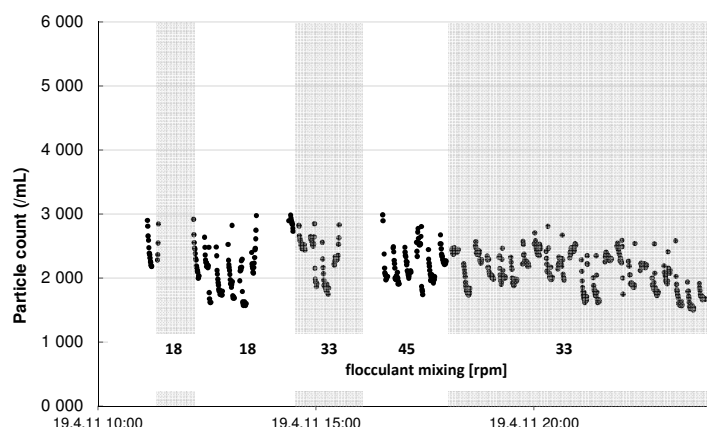


**Figure 32: Increase of the mixing velocity in the flocculation tank**

This trial showed the best results at 45 rpm: the total particle concentration was low (around 2000 – 3000) and the backwash time (65%) was the lowest. The other parameters such as the turbidity and the total phosphorus concentration in the effluent were not able to give valuable information. The higher the mixing velocity; the lower was the backwash time. With a higher mixing velocity, the flocs were stronger and able to withstand the high shear force during the filtration. It was not possible to test a mixing velocity above 45 rpm to find an optimum but it is recommended to operate the pilot plant with a higher rotation speed. This case shows the value and the reliability of the online particle counter device to optimize a process such as a microsieve filtration.

#### 4.4.5.3 Flocculation hydraulic retention time

No impact of the hydraulic retention time (HRT) in the flocculation tank was observed in the particle concentration in the effluent water. However more post flocculation could be seen in the pilot plant effluent pipes. The assumption is that the HRT was too low to build strong flocs and therefore more particles and chemicals could flow through the filter. Another indicator was the increase of the backwash time.

### 4.5 Operational experiences

The particle counter from Pamas worked with a high reproducibility and reliability online with a high frequency measurement. The highest error source was not the device but the way to get a representative sample into the sensor cell. Accumulation of particles occurred rapidly in pipes leading to the measurement device (see Figure 33).



**Figure 33: Particle counter piping system fouled**

To limit this fouling effect, automatic cleaning took place every 30 minutes but was not always efficient enough. Moreover the cleaning solution: distilled water or distilled water with 1% HCl had to be changed at least daily. Additionally, mechanical cleaning was needed for the pipes and for the sensor cell on a weekly basis. For the pipes, a syringe filled with distilled water or air was connected and pushed the foulants away manually. For the sensor cell, the device had to be dismantled and then the cell was cleaned with high pressure air.

This device maintenance is time consuming. In comparison the turbidity sensor had to be cleaned 2 to 3 times a week.

It can also lead to comparability issues between samples measured directly after cleaning and samples measured directly before cleaning. After cleaning, fewer particles are accumulated to the pipe wall, meaning that fewer large particles can be entrapped with foulants and more will arrive at the sensor cell. A small pipe diameter means than fewer large particles from the sample will be measured by the device, but a large pipe diameter means a lower sample flow. A compromise has to be found between a high flow (high shear force = less accumulation) and larger pipe diameter. It is also recommended to reduce the length between the sampling point and the sensor cell.

#### **4.6 Conclusion on online monitoring of microsieve performance**

In this study the treated domestic wastewater quality during microsieve filtration ( $10\text{ }\mu\text{m}$ ) was investigated by sizing and counting the particles between 1 and  $200\text{ }\mu\text{m}$  using an optical particle counter: the PAMAS WaterViewer. The goal was to find a link between the pre-treatment (coagulation and flocculation) characteristics, the filtration parameters such as mesh size, rotational velocity and the process performance. A pre-treatment by coagulation and flocculation had to be optimized in order to improve the floc strength and size before the  $10\text{ }\mu\text{m}$  filtration to achieve the best possible effluent water quality. An online installation of the instrument was conducted to investigate its potential for real-time process optimization such as adaptation of chemicals doses and mixing velocity, depending on the effluent particle concentration detected by the particle counter. Particle analysis by the WaterViewer was obtained to give reliable and reproducible information about the concentration and size distributions of the tested treated domestic wastewater.

To detect the main absolute particle size of the sample, particle counter results were evaluated using particle volume distribution curves. To detect the influence of process parameters on the effluent water quality, particle counter results were evaluated using particle size distribution. The particle concentration for different particle size ranges was measured per mL of sample analysed. The differential distribution shows the relative particle amount in each particle size range. The WaterViewer can detect up to eight different size ranges. However, the particle concentration variations were often the same in all size ranges. Therefore in this report the total particle count was more frequently interpreted. A consistent detection of variations in particle concentration after coagulation with polyaluminium chloride and flocculation with a high molecular weight cationic polymer was carried out in a range between 1000 and 6000 particles / mL. Around 90% of particles between 0 and  $10\text{ }\mu\text{m}$  were removed after a  $10\text{ }\mu\text{m}$  filtration.

Performance of the installed particle counter were compared with performance of a standard and well known online turbidity sensor. This study results showed a higher sensitivity from the particle counter most of the time. It could detect change in the inflow: at constant influent turbidity a higher particle count were detected for higher flows, although the effluent turbidity stayed constant. Another typical example is the optimization of coagulation and flocculation mixing velocity. The particle counter detected the lowest particle concentration for the optimized G-value whereas the turbidity sensor did not detect any changes. Particle count results variations were also observed in the effluent water quality after flocculation with two different polymer types or after filtration with different filter mesh sizes even though no other parameters could see these variations. This device proves itself to be valuable for process optimization.

Under stable operating conditions, results of the online particle counter were very similar to the online turbidity sensor ones. The performance of both instruments depends on the cleaning frequency of the pipes and sensor cells. However the maintenance effort is lower for the online turbidity sensors. After coagulation, flocculation and filtration at  $10\text{ }\mu\text{m}$  residual coagulant and flocculant provokes “post-flocculation” in the instrument piping. Particles agglomerated themselves and obstructed the way between the sampling point and the measuring cell which diminishes the accuracy of the particle counter.

To conclude, we would recommend the use of an online optical particle counter to optimize a process such as a microsieve pilot plant especially during the start-up phase. However as soon as the process is optimized and needs only routine control, it is recommended to use an online turbidity sensor to control the effluent water quality which provides similar results to the particle counter and are less demanding in terms of maintenance effort.

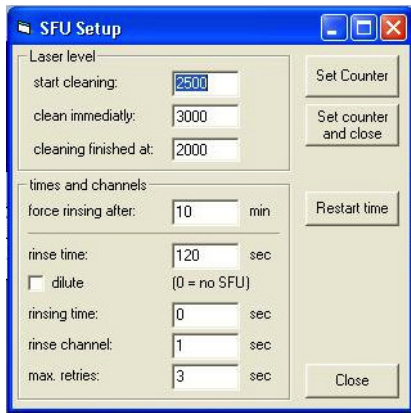
## Appendix A Software options

### Options to program measurement series:

- pre-run: time duration to pump sample without measuring the particle size and number before each measurement series
- sample time: time duration of the measurement
- sample delay: time duration between the measurement series
- runs/set: Number of measurements per measurement series

### Options to program the Sensor Flushing unit (SfU) :

The automatic cleaning takes place during operation, initiated either after a defined time or at a defined sensor level – a value describing the status of the sensor. Both can be controlled by going to: **Tools > SFU setup**



## Appendix B Fouling analysis

Resistance is defined as the counteracting of the membrane and the fouling against feed water flux. Total resistance includes membrane resistance, reversible resistance and irreversible resistance and was calculated according to Darcy's law:

### equation 2: Darcy's law

$$J = \frac{\Delta p}{\eta \cdot R_f} = \frac{\Delta p}{\eta \cdot (R_m \cdot R_{rev} \cdot R_{irr})}$$

$R_m$  = membrane resistance [ $m^{-1}$ ]  
 $R_{rev}$  = reversible fouling resistance [ $m^{-1}$ ]  
 $R_{irr}$  = irreversible fouling resistance [ $m^{-1}$ ]

Initial membrane resistance  $R_{m,0}$  is calculated with the pure water flux for the lab scale experiments:

### equation 3: initial membrane resistance

$$R_{m,0} = \frac{\Delta p}{\eta \cdot J_0}$$

$R_{m,0}$  = initial (clean) membrane resistance [ $m^{-1}$ ]  
 $J_0$  = pure water flux [ $L m^{-2} h^{-1}$ ]

Total fouling resistance  $R_{d,n}$  of filtration cycle n is determined as the difference between filtration resistance  $R_f$  and membrane resistance  $R_{m,n-1}$  at the start of the cycle:

### equation 4: total fouling resistance

$$R_{d,n} = \frac{\Delta p}{\eta \cdot J_{end,n}} - \frac{\Delta p}{\eta \cdot J_{n-1}}$$

$R_{d,n}$  = total fouling resistance cycle n [ $m^{-1}$ ]  
 $J_{end,n}$  = flux at the end of cycle n [ $L m^{-2} h^{-1}$ ]

Specific irreversible fouling resistance  $R_{irr,n}$  of filtration cycle n defines the fouling, which cannot be removed by hydraulic backwash and is calculated as follows:

### equation 5: irreversible fouling

$$R_{irr,n} = \frac{\Delta p}{\eta \cdot J_n} - \frac{\Delta p}{\eta \cdot J_{n-1}}$$

$R_{irr,n}$  = irreversible fouling resist. cycle n [ $m^{-1}$ ]  
 $J_n$  = pure water flux after backwash n [ $L m^{-2} h^{-1}$ ]

Specific reversible fouling resistance  $R_{rev,n}$  of filtration cycle n is calculated by:

### equation 6: reversible fouling

$$R_{rev,n} = \frac{\Delta p}{\eta \cdot J_{end,n}} - \frac{\Delta p}{\eta \cdot J_n}$$

$R_{rev,n}$  = reversible fouling resist. cycle n [ $m^{-1}$ ]

For pilot-scale investigations, initial membrane resistance was not calculated, as the plant was not operated with pure water. Total fouling resistance as well as the portion of reversible and irreversible resistance was calculated similarly, with the only difference that, in case of constant flux operation, the trans-membrane pressure ( $\Delta p$ ) is variable. Indices of the equations have to be transformed to the pressure term, while the flux keeps constant. TMP values at the start and the end of a cycle were averaged about 2 min to get reliable values.

Fouling rate is an additional parameter, which quantifies the long term fouling at pilot-scale investigation. It is defined as the increase of membrane resistance  $R_m$  as a function of time:

**equation 7: fouling rate**

$$\frac{dR_m}{dt} = \left( \frac{\Delta p_{n+k(t)}}{\eta \cdot J} - \frac{\Delta p_n}{\eta \cdot J} \right) \cdot \frac{1}{dt}$$

$\Delta p_n = \text{TMP after BW at start of time period}$   
 $[bar]$   
 $\Delta p_{n+k(t)} = \text{TMP after BW at end of period [bar]}$

## Appendix C Scattering intensity

For NTA, besides the diffusion velocity of each colloid, the scattering intensity is recorded as the magnitude of light which is scattered by the colloid surface. On the one hand, this intensity depends on the size of the colloid. Colloids with larger diameter are able to scatter more light due to a higher surface area. On the other hand, the surface properties are influence the sum of scattered light. Inorganic colloids have a higher scattering intensity, due to a more homogenous surface, whereas organic colloids or those with an organic-coating absorb a part of the emitted light and lower intensity values will be detected. This allows a rough classification of the nature of colloids present in the sample. A scattering intensity analysis was conducted, where the intensity signal of a secondary effluent sample was compared to several particle standards of different materials (gold, polystyrene, latex) analyzed under similar conditions (Figure 34). The analysis of particle standards shows a linear trend between particle size and the scattering intensity of the same particle material. Highest intensities are determined for gold standards, followed by polystyrene standard particles, whereas latex scatters the lowest amount of light.

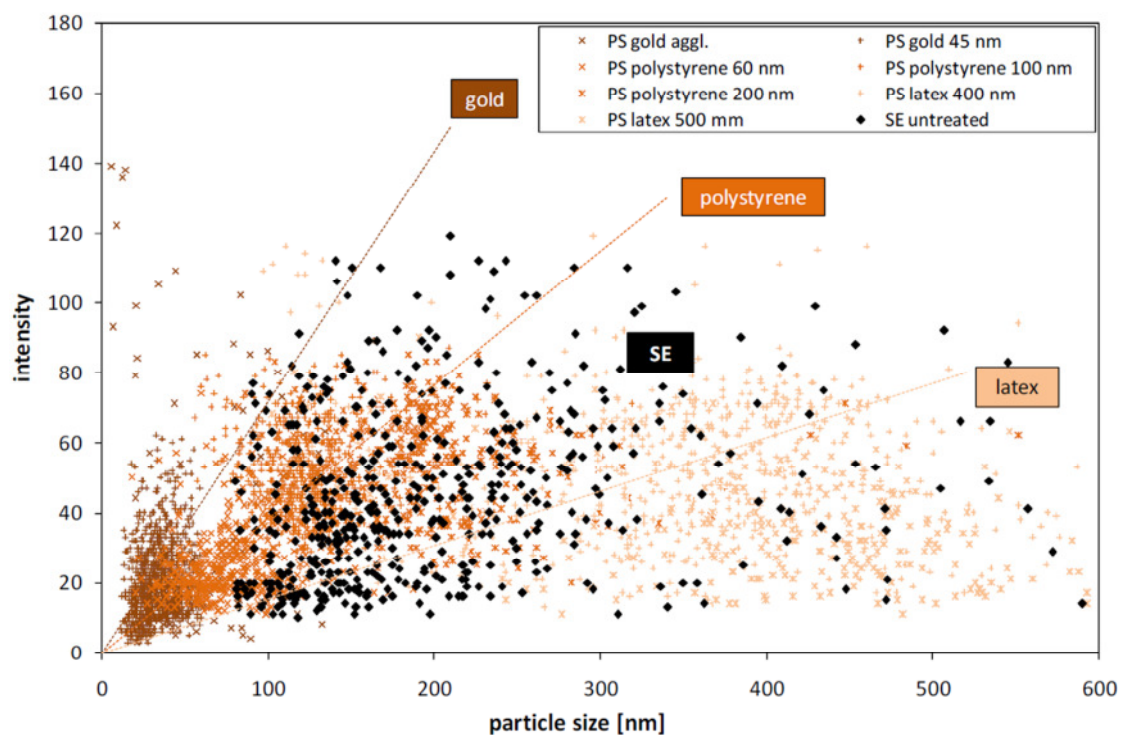


**Figure 34: Relation between particle size and scattering intensity of different particle standard (PS) materials compared to intensity signal of a secondary effluent (SE) sample**

Treated domestic wastewaters contain an inhomogeneous mixture of colloids of different origin and chemistry. Besides inorganic compounds, like silicates, carbonates and metal hydroxides, a large amount of organic colloids of all size fractions are expected to be present in a secondary effluent. Boller (2007) determined that for treated wastewaters with applied P-precipitation, 55 % of submicron particles are organic, whereas the rest are inorganic, including 8-9 % ferric colloids formed by precipitation. However, inorganic solid surfaces are coated by organic compounds due to the high amount of organic matter in treated domestic wastewaters (see chapter 2.1.3 DA MS). The secondary Ruhleben effluent was obtained containing a broad range

of colloid sizes with large variations of scattering intensity (Figure 34). A very inhomogeneous distribution of intensity rates was observed in the sample, which may indicate the presence of inorganic as well as organic colloids. The bulk of submicron particles have lower intensity rates in the range of latex particles or below, which suggests that they are of organic nature or are coated by dissolved organic substances. However, a part of submicron particles is found at intensity ranges far above the intensity of polystyrene, which could possibly be of geological origin, like silicates or clays, or residuals of the simultaneous P-precipitation in the biological purification stage. The intensity data must be interpreted with caution. Intensity values are given on a relative, instrument specific scale, without a unit. It allows a rough assessment on the surface structure of colloids, but no real classification. Tests with various standard materials (e.g. silicates, organic nano-flocs) of different sizes would be necessary to allow a more detailed characterization of the composition of the submicron particle fraction of this secondary effluent. This was not possible within the scope of this study. However, a relative comparison can be conducted between different samples by the use of intensity data. Hence, for example the impact of ozonation and coagulation on submicron particles of different chemistries can be investigated.

## Bibliography

- Alasonati, E., Slaveykova, V.I. , Gallard, H., Croué, J.-P., Benedetti, M.F. (2010): Characterization of the colloidal organic matter from the Amazonian basin by asymmetrical flow field-flow fractionation and size exclusion chromatography. *Water research* 44 (1), 223-231.
- Amirtharajah, A., Mills, Kirk M. (1982): Rapid-mix design for mechanisms of alum coagulation. *Journal / American Water Works Association* 74 (4), 210-216.
- Amy, G. (2008): Fundamental understanding of organic matter fouling of membranes. *Desalination* 231, 44-51.
- Baalousha, M., Lead, J.R. (2007): Size fractionation and characterization of natural aquatic colloids and nanoparticles. *Science of the Total Environment* 386 (1-3), 93-102.
- Bache, D. H. and Gregory, R. (2007). Flocs in water treatment. UK.
- Bache, D.H., Gregory, R. (2010): Flocs and separation processes in drinking water treatment: A review. *Journal of Water Supply: Research and Technology - AQUA* 59 (1), 16-30.
- Becker, C.B. and O'Melia, C.R. (1996): Ozone, oxalic acid and organic matter molecular weight effects on coagulation. *Ozone Science & Engineering* 18, 311-324.
- Boulestreau, M. and Miehe, U. (2009): Review on monitoring techniques for fouling and flocculation mechanisms and recommendations to monitor tertiary filtration processes on on-line monitoring. Report, Projekt OXERAM D3.2. Kompetenzzentrum Wasser Berlin, Germany.
- Boulestreau, M. and Miehe, U. (2009): State of the art of the effect of coagulation and ozonation on membrane fouling. Report, Projekt OXERAM D3.3. Kompetenzzentrum Wasser Berlin, Germany.
- Carr, B., Hole, P., Malloy, A., Nelson, P., Wright, M. and Smith, J. (2009): Applications of nanoparticle tracking analysis in nanoparticle research – a mini-review. *European Journal of Parenteral & Pharmaceutical Sciences* 14(2), 45-50.
- Chandrakanth, M.S. and Amy, G.L. (1996): Effects of ozone on the colloidal stability and aggregation of particles coated with natural organic matter. *Environmental Science & Technology* 30, 431-443.
- Chen, V., Li, H., and Fane, A. G. (2004): Non-invasive observation of synthetic membrane processes – a review of methods. *Journal of Membrane Science* 241, 23–44.
- Cheryan, M. (1988): Ultrafiltration in food and bioprocessing. Lancaster, PA: Technomic Publishing.
- Citulski, J., Farahbakhsh, K., Kent, F. and Zhou, H. (2008). The impact of in-line coagulant addition on fouling potential of secondary effluent at a pilot-scale immersed ultrafiltration plant. *Journal of Membrane Science* 325: 311-318.

- Crittenden, J.C., Trussell, R.R., Hand, D.W., Howe, K.J. and Tchobanoglous G. (2005): Water Treatment: Principles and Design. Second Edition, John Wiley & Sons, Inc., New Jersey, U.S.A.
- DVGW (1998): (DVGW): Flockung in der Wasseraufbereitung – Flockungstestverfahren. Deutsche Vereinigung des Gas- und Wasserfaches e.V.. Worksheet W 218, Bonn, Germany.
- Edwards, M., Benjamin, M.M. and Tobias, J.E. (1994): Effects of ozonation on coagulation of NOM using polymer alone and polymer/metal salt mixture. Journal of American Water Works Association 86, 105-116.
- Filipe, V., Hawe, A. and Jiskoot, W. (2010): Critical evaluation of Nanoparticle Tracking Analysis (NTA) by NanoSight for measurement of nanoparticles and protein aggregates. Pharmaceutical Research 27, 796-810.
- Filloux, E. (2006): Urban wastewater reuse: fouling of low pressure membrane by effluent organic matter. Doctoral thesis.
- Genz, C., Miehe, U., Gnirß, R. and Jekel, M. (2011): The effect of pre-ozonation and subsequent coagulation on the filtration of WWTP effluent with low pressure membranes. Water Science & Technology, (submitted).
- Gimbert, L. J., Haygarth, P. M., Bol, R., and Worsfold, P. J. (2009): Temporal variability of colloidal material in agricultural storm runoff from managed grassland using flow field-flow fractionation. Journal of Chromatography A.
- Gregory, J. (2004): Monitoring floc formation and breakage. Water science and technology 50, 163-170.
- Haberkamp, J., Ruhl, A.S., Ernst, M. and Jekel, M. (2007): Impact of coagulation and adsorption on DOC fractions of secondary effluent and resulting fouling behavior in ultrafiltration. Water Research 41, 3794-3802.
- Haberkamp, J. (2008): Organisches Membranfouling bei der Ultrafiltration kommunaler Kläranlagenablüfe: Ursachen, Mechanismen und Massnahmen zur Verringerung. PhD-Thesis, Technische Universität Berlin, Germany.
- Hofmann, T., Kammer, F. vd (2009): Estimating the relevance of engineered carbonaceous nanoparticle facilitated transport of hydrophobic organic contaminants in porous media. Environmental Pollution 157 (4), 1117-1126.
- Jekel, M. (1986a): Interactions of humic acids and aluminium salts in the flocculation process. Water Research 20, 1535-1542.
- Jekel, M. (1986b): The stabilization of dispersed mineral particles by adsorption of humic substances. Water Research 20, 1543-1554.
- Jekel, M. R. (1998). Effects and mechanisms involved in preoxidation and particle separation processes. Water Science & Technology 37(10): 1-7.
- Jekel, M. (2000): Full-Scale Applications. Ozonation of Water and Waste Water. C. Gottschalk, J. A. Libra and A. Saupe. WILEY-VCH, Weinheim, Germany.

- Jekel, M. (2004): Flockung, Sedimentation und Flotation. In: Wasseraufbereitung–Grundlagen und Verfahren. DVGW Lehr- und Handbuch Wasserversorgung Vol. 6., Gimbel, R., Jekel, M. und Liessfeld, R. (Eds.), Oldenbourg Industrieverlag, München/Wien.
- Jermann, D., Pronk, W., Meylan, S. and Boller M. (2007): Interplay of different NOM fouling mechanisms during ultrafiltration for drinking water production. *Water Research*, 41, 1713–1722.
- Kim, S-H., Moon, S-Y., Yoon, C-H., Yim, S-K., Cho, J-W. (2005): Role of coagulation in membrane filtration of wastewater for reuse. *Desalination* 173 (3), 301-307.
- Kim, H.-C and Dempsey, B.A. (2008): Effects of wastewater effluent organic materials on fouling in ultrafiltration. *Water Research* 42, 3379-3384.
- Langer, M. and Schermann, A. (2013): Feasibility of the microsieve technology for advanced phosphorus removal. Report, Projekt OXERAM D5.2. Kompetenzzentrum Wasser Berlin, Germany.
- Langlais, B., Reckhow, D. A., Brink, D. R. (1991): Ozone in Water treatment: Application and engineering. American Water Works Association Research Foundation: Compagnie Générale des Eaux.
- Leiknes, T. O. (2009). "The effect of coupling coagulation and flocculation with membrane filtration in water treatment: A review." *Journal of Environmental Sciences* 21, (1), 8-12.
- Lipp, P., Baldauf, G. and Hetzer, B. (2009). Methode zur Ermittlung des Foulingpotenzials bei der Ultrafiltration (UF-FP). *Forschung und Entwicklung*. Karlsruhe: 58-61.
- Liu, H., Cheng, F. and Wang, D. (2009): Interaction of ozone and organic matter in coagulation with inorganic polymer flocculant-PACl: Role of organic components. *Desalination* 249, 596-601.
- Ljunggren, M., Jönsson, L., and la Cour Jansen, J. (2004): Particle visualisation- a tool for determination of rise velocities. *Water science and technology* 50, 229-236.
- Meier, P., Salehi, F., Kazner, C., Wintgens, T. and Melin, T. (2006). Ultrafiltration with pre-coagulation in drinking water production – Literature review, Techneau D5.3.4a.
- Melin, T., and Rautenbach, R. (2004): Membranverfahren Grundlagen der Modul- und Anlagenauslegung. Aachen.
- Melin, T. and Rautenbach, R. (2007): Membranverfahren Grundlagen der Modul- und Anlagenauslegung, 3rd. Edition. Springer, Berlin Heidelberg New York.
- Moulin, C. (1990). Potabilisation d'une eau de surface par filtration tangentielle sur membranes minérales: étude de traitements physico-chimiques associés. . Université des Sciences et Techniques du Languedoc. Montpellier, Université de Montpellier II: 164.
- NAN, J., HE, W., SONG, X. and LI, G. (2008). "Impact of dynamic distribution of floc particles on flocculation effect."

- NanoSight (2010a): Direct visualization, sizing and counting of aggregations in proteins. Application Note, [www.nanosight.com](http://www.nanosight.com), 08/04/2010. Nanosight Ltd, Amesbury, UK.
- NanoSight (2010b): Nanoparticle Tracking Analysis (NTA) and Dynamic Light Scattering (DLS) – a comparison. Application Note, [www.nanosight.com](http://www.nanosight.com), 14/04/2010. Nanosight Ltd, Amesbury, UK.
- NanoSight (2010c): NanoSight NTA 2.1 Analytical Software – Operating Manual. Version 1.0. Nanosight Ltd, Amesbury, UK.
- Nieuwenhuijzen, A.F. van, Graaf, J.H.J.M. van der, and Mels, A.R. (2003): Particle related fractionation and characterization of municipal wastewater. In: IWA specialist conference on Nano and Microparticles in Water and Wastewater Treatment - Conference proceedings. 22 - 24 September 2003. Zurich, Switzerland.
- Nieuwenhuijzen A. Van, Graaf J.H.J.M van der, (2011): Handbook on particle separation processes, IWA Publishing.
- Plume, S. (2010): In-line Flockung vor der Ultrafiltration von kommunalem Kläranlagenablauf zur Verringerung von Membranfouling und zur Entfernung von Phosphor. Diploma thesis at the chair of Water Quality Control, Technische Universität Berlin, Germany.
- Potts, D. E., Ahlert, R. C., and Wang, S. S. (1981): A critical review of fouling of reverse osmosis membranes. Desalination, 36 (3), 235-264.
- Richard, Y. and Brener, L. (1980): Interference Dioxyde de chlore: ozone en traitement d'eau de consummation. Conference in Strasbourg.
- Roustan, M., Mallevialle, J., Roques, H. and Jones, J. P. (1980). "Mass transfer of ozone to water a fundamental study." Ozone: Science and engineering 2(4): 337-344.
- Schulz, M. (2012): Submicron particle analysis to characterize fouling in tertiary membrane filtration. Master thesis, Projekt OXERAM Kompetenzzentrum Wasser Berlin, Germany.
- Singer, P. C. 1990. Assessing ozonation research needs in water treatment. Journal / American Water Works Association 82 (10): 78-88.
- Soun-Ok Baek, I.-S. C. (2009). "Pretreatments to control membrane fouling in membrane filtration of secondary effluents." Desalination 244: 153-163.
- Stoller, M. (2009). "On the effect of flocculation as pretreatment process and particle size distribution for membrane fouling reduction." Desalination 240: 209-217.
- Wu, J. and He, C. (2010): Experimental and modeling investigation on sewage solids sedimentation based on particle size distribution and fractal dimension. International Journal of Environmental Science and Technology 7(1), 37-46.
- You, S.-H., Tseng, D.-H. and Hsu, W.-C. (2007). Effect and mechanism of ultrafiltration membrane fouling removal by ozonation. Desalination 202 224–230.

Zheng, X., Ernst, M., and Jekel, M. (2009): Identification and quantification of major organic foulants in treated domestic wastewater affecting filterability in dead-end ultrafiltration. Water research 43, 238-244.

Zhu, H.T., Wen, X.H. and Huang, X. (2008): Pre-ozonation for dead-end microfiltration of the secondary effluent: suspended particles and membrane fouling. Desalination 231, 166-174.